IOPscience iopscience.iop.org

Home Search Collections Journals About Contact us My IOPscience

A smoothing spline that approximates Laplace transform functions only known on measurements on the real axis

This content has been downloaded from IOPscience. Please scroll down to see the full text.

2012 Inverse Problems 28 025007

(http://iopscience.iop.org/0266-5611/28/2/025007)

View the table of contents for this issue, or go to the journal homepage for more

Download details:

IP Address: 192.133.28.4
This content was downloaded on 09/02/2016 at 10:45

Please note that terms and conditions apply.

IOP PUBLISHING INVERSE PROBLEMS

Inverse Problems **28** (2012) 025007 (37pp) doi:10.1088/0266-5611/28/2/025007

A smoothing spline that approximates Laplace transform functions only known on measurements on the real axis

L D'Amore[1], R Campagna[1], A Galletti[2], L Marcellino[2] and A Murli[1]

[1] Department of Mathematics and Applications, University of Naples Federico II, Via Cintia, Naples, Italy
[2] Department of Applied Sciences, University of Naples Parthenope, Centro Direzionale, Naples, Italy

E-mail: luisa.damore@unina.it, rosanna.campagna@unina.it, ardelio.galletti@uniparthenope.it, livia.marcellino@uniparthenope.it and almerico.murli@unina.it

Received 17 January 2011, in final form 15 November 2011
Published 13 January 2012
Online at stacks.iop.org/IP/28/025007

Abstract

The scientific and application-oriented interest in the Laplace transform and its inversion is testified by more than 1000 publications in the last century. Most of the inversion algorithms available in the literature assume that the Laplace transform function is available everywhere. Unfortunately, such an assumption is not fulfilled in the applications of the Laplace transform. Very often, one only has a finite set of data and one wants to recover an estimate of the inverse Laplace function from that. We propose a fitting model of data. More precisely, given a finite set of measurements on the real axis, arising from an unknown Laplace transform function, we construct a dth degree *generalized polynomial smoothing spline*, where $d = 2m-1$, such that internally to the data interval it is a dth degree polynomial complete smoothing spline minimizing a regularization functional, and outside the data interval, it mimics the Laplace transform asymptotic behavior, i.e. it is a rational or an exponential function (the *end behavior model*), and at the boundaries of the data set it joins with regularity up to order $m-1$, with the end behavior model. We analyze in detail the generalized polynomial smoothing spline of degree $d = 3$. This choice was motivated by the (ill)conditioning of the numerical computation which strongly depends on the degree of the complete spline. We prove existence and uniqueness of this spline. We derive the approximation error and give *a priori* and computable bounds of it on the whole real axis. In such a way, the generalized polynomial smoothing spline may be used in any real inversion algorithm to compute an approximation of the inverse Laplace function. Experimental results concerning Laplace transform approximation, numerical inversion of the generalized polynomial smoothing spline and comparisons with the exponential smoothing spline conclude the work.

(Some figures may appear in colour only in the online journal)

 © 2012 IOP Publishing Ltd Printed in the UK & the USA

1. Introduction

In many applications of the Laplace transform (Lt) inversion, the observed data are related to the inverse function only by a finite amount of data (often measurements) on the Lt. Very often, the Lt function is unknown [7, 30–32]. As expected, the fact that the Lt is only known on a finite set of points on the real axis makes the inversion problem much more difficult. The approaches that can be found in the literature attempt to find a constrained least-squares solution minimizing the residual together with some additional constraints [2, 14]. The limit of these methods mainly consists of the numerical difficulty of the inversion procedure for a finite amount of experimental data.

We propose to construct a *fitting* model of the data set. Such a model may be employed in any inversion method able to compute the inverse Laplace function in the real case. Let us describe the mathematical problem that we are going to address.

$\mathcal{P}_1$: *given a finite set of real values* $x_i \in \Delta_n$ *where*

$$\Delta_n = \{x_1 < x_2 < \cdots < x_n\} \subset \mathrm{Re}^+, \tag{1}$$

let F *be a Lt function defined on the half-plane of convergence* $\mathcal{HC} = \{s \in \mathcal{C} : \mathrm{Re}(s) > \sigma_0\}$,[3] *where* $\sigma_0 \geqslant 0$ *is the abscissa of convergence of* F.

Let us assume that F *is only given at*

$$x_i \in \Delta_n \subset (\mathrm{Re}^+ \cap \mathcal{HC}), \qquad i = 1, ..., n, \tag{2}$$

and $(y_i)_{i=1,...,n}$ *be* n *measurements of* F *at* $(x_i)_{i=1,...,n}$. *Moreover, let* $x_{n+1} = +\infty$. *We deal with the inverse problem concerning the construction of an approximation of* F *on the whole real axis starting from the data set* (x_i, y_i), $i = 1, \ldots, n$.

A number of papers have been written for data smoothing [8, 13, 16, 25, 28]. One of the most effective ways to do this is by using spline functions [5, 10, 15, 17–19, 26, 27]. Natural splines are well known and widely used in many applications; unfortunately, these functions do not do well near the boundary of the data set because the second-order derivative of natural splines at the end points are zero. Better results can be obtained if one requires that the regularity of the spline and its derivatives at the boundaries of the data set be equal to known values. Splines which fit data with constraints on their derivatives at the boundaries of the data set are called *complete splines* [4, 6]. In the special case of interpolation at all integers, i.e. $x_i = i$, $i = 0, \pm 1, \pm 2, \ldots$, the so-called *polynomial cardinal splines* have been extensively studied and are the subject of a monograph by Shoenberg [19]. The existence and uniqueness results regarding the interpolation problem using the *polynomial cardinal spline* were generalized by Micchelli [11], to the *cardinal L-spline*, where L is a differential operator with constant real coefficients. Finally, the Shoenberg one-dimensional cardinal splines were extended in Re^n by Kounchev, who in [9] introduced the piecewise polyharmonic splines (the so-called *polysplines*). Polysplines are multivariate splines made up of polyharmonic functions that allow us to interpolate functions prescribed on surfaces of co-dimension 1.

In our preliminary results [3], we used a complete spline interpolating the data set with a rational asymptotic decay. Here, starting from n measurements (x_i, y_i), $i = 1, \ldots, n$, we construct a dth degree *generalized polynomial smoothing spline*[4], where $d = 2m - 1$, such that internally to the data interval it is a dth degree polynomial complete smoothing spline solution of a regularization problem, and outside the data interval, it mimics the Lt asymptotic behavior, i.e. it is a rational or an exponential function (the *end behavior model*), and at the

[3] $\mathcal{C}$ denotes the complex plane.

[4] From now on, we refer to the *polynomial splines* also simply as *splines.*

boundaries of the data set it joins with regularity up to order $m-1$, with the end behavior model. The selection of the former or of the latter end behavior model may be done according to information *a priori* that we have on the observed data or on the inverse function. For instance, taking into account Abelian/Tauberian results, if we estimate the behavior of the inverse function at zero, we can use this information to choose the end decay of the generalized polynomial smoothing spline.

We address in detail the generalized polynomial smoothing spline of degree $d = 3$. This choice was motivated by the (ill)conditioning of the numerical computation which strongly depends on the degree of the complete spline. We prove existence and uniqueness of the generalized spline. Moreover, the error analysis is carried out together with *a priori* and computable bounds of the approximation error between the generalized smoothing spline and the n measurements. It is worth noting that the generalized smoothing spline can be constructed using, internally to the data interval, spline functions which are different from the polynomial splines. For instance, we report some comparisons with the generalized exponential smoothing spline, obtained by using the exponential splines as described in [22].

The organization of the paper is as follows. In section 2, we give some preliminary definitions, according to the asymptotic behavior of a Lt function, and we introduce the set of functions with *asymptotic rational decay* and the set of functions with *asymptotic exponential decay*. Section 3 is devoted to the definition of the fitting model, and to its existence and uniqueness. In section 4, we study the approximation error and give *a priori* and *computable* bounds. Section 5 is devoted to the round-off error propagation during the construction and evaluation of the spline model. In order to show the usefulness of this approach, experiments concerning the numerical inversion of the generalized smoothing spline and comparisons with another fitting spline are given in section 6. Conclusions and future works are discussed in section 7.

2. Preliminaries

Let $\Omega \subseteq \mathrm{Re}^+$ such that $[c, \infty[\subset \Omega$ for a constant $c > 0$. Let $\mathcal{T}(\Omega)$ be the set of analytic functions on $\Omega \subseteq \mathrm{Re}^+$.

Definition 2.1. *If $\alpha > 0$, then the function space*

$$\mathcal{R}^{\alpha}_{\mathrm{decay}}(\Omega) = \left\{ \begin{array}{ll} & \exists\, H(x) = a_1 x^{-\alpha} + a_2 x^{-(\alpha+\delta)} \\ G \in \mathcal{T}(\Omega): & a_1, a_2, \delta \in \mathrm{Re},\ \ a_1 \neq 0,\ \delta > 0 \text{ s.t.} \\ \text{for } x \to \infty, & G^{(k)}(x) = H^{(k)}(x) + o\left(x^{-(\alpha+\delta+k)}\right) \\ & \text{for } k = 0, 1, \ldots \end{array} \right\} \tag{3}$$

denotes functions with the rational decay of order α on Ω.

Definition 2.2. *If $\alpha > 0$, then the function space*

$$\mathcal{E}^{\alpha}_{\mathrm{decay}}(\Omega) = \left\{ \begin{array}{l} G \in \mathcal{T}(\Omega) : \exists \text{ a bounded function } H(x) \text{ defined on } \Omega \\ \text{s.t.} G(x) = \mathrm{e}^{-\alpha x} H(x) \end{array} \right\} \tag{4}$$

denotes functions with exponential decay of order α in Ω.

Let $\mathcal{S}_d(\Delta_n)$ be the space of (polynomial) dth degree splines defined on Δ_n, then

Definition 2.3 [4]**.** *Let $m > 0$ be a positive integer, $d = 2m-1$, and $\{S^i_L\}_{i=1,\ldots,m-1}$, $\{S^i_R\}_{i=1,\ldots,m-1}$ $2m-2$ real numbers. If $s \in \mathcal{S}_d(\Delta_n)$ satisfies the following properties:*

$$\begin{aligned} s^{(i)}(x_1) &= S^i_L, \quad i = 1, \ldots, m-1 \\ s^{(i)}(x_n) &= S^i_R, \quad i = 1, \ldots, m-1, \end{aligned} \tag{5}$$

then s is said to be a complete dth degree spline. The space of complete dth degree splines is denoted by $\mathcal{S}_{\mathrm{com},d}(\Delta_n, S_L^i, S_R^i)$. *Moreover, if s satisfies the following property:*

- $s(x_i) = y_i$, $i = 1, \ldots, n$,

then $s(x)$ *is said to be a complete dth degree spline interpolating* $(x_i, y_i)_{i=1,\ldots,n}$, $\{S_L^i, S_R^i\}_{i=1,\ldots,m-1}$.

Let $L_2^m[x_1, x_n] = \{f \in C^{m-1}[x_1, x_n] : f^{(m-1)}$ be absolutely continuous and $f^{(m)} \in L_2[x_1, x_n]\}$ and consider the following functional:

$$E(f) = \sum_{i=1}^{n} w_i[f(x_i) - y_i]^2 + \sum_{i=1}^{m-1} w_i^L\big[f^{(i)}(x_1) - S_L^i\big]^2 + \sum_{i=1}^{m-1} w_i^R\big[f^{(i)}(x_n) - S_R^i\big]^2, \tag{6}$$

where $\{w_1, \ldots, w_n\}$, $\{w_1^L, \ldots, w_{m-1}^L\}$ and $\{w_1^R, \ldots, w_{m-1}^R\}$ are positive weights, and let

$$J(f) = \int_{x_1}^{x_n} (f^{(m)}(t))^2 \mathrm{d}t. \tag{7}$$

To solve the inverse problem $\mathcal{P}_1$, we introduce the *regularization problem* $\mathcal{P}_2$:

$$\text{minimize } \{\rho J(f) + E(f)\} \text{ over } f \in L_2^m[x_1, x_n], \tag{8}$$

where $\rho \geqslant 0$ is the so-called *regularization parameter* controlling the weight of $J(f)$ with respect to $E(f)$.

If $\rho = 0$, then problem (8) has a unique solution which is just the complete $(2m-1)$th degree spline interpolating $(x_i, y_i)_{i=1,\ldots,n}$, $\{S_L^i, S_R^i\}_{i=1,\ldots,m-1}$, while, for each choice of $\rho > 0$, the unique solution is a $(2m-1)$th degree spline.

Theorem 2.4 [4]**.** *Let* $m > 0$ *be a positive integer and* $d = 2m - 1$. *For every given data set,*

$$\{(x_i, y_i)\}_{i=1,\ldots,n}, \quad \big\{S_L^i\big\}_{i=1,\ldots,m-1}, \quad \big\{S_R^i\big\}_{i=1,\ldots,m-1}, \tag{9}$$

for every given set of positive weights

$$\{w_i\}_{i=1,\ldots,n}, \quad \big\{w_i^L\big\}_{i=1,\ldots,m-1}, \quad \{w_i^R\}_{i=1,\ldots,m-1} \tag{10}$$

and for every choice of the regularization parameter $\rho > 0$, *the problem (8) has a unique solution. This solution is a dth degree spline denoted by* $s_\rho \in \mathcal{S}_d(\Delta_n)$.

As $\rho \to \infty$, *the function* s_ρ *converges to the polynomial of degree* $m-1$ *which fits data* $(x_i, y_i)_{i=1,\ldots,n}$ *best in the least-squares sense.*

As $\rho \to 0$, *the function* s_ρ *converges to the dth degree complete spline interpolating* $(x_i, y_i)_{i=1,\ldots,n}$, $\{S_L^i, S_R^i\}_{i=1,\ldots,m-1}$.

As in [4] we give the following.

Definition 2.5. *The unique solution* s_ρ *of the regularization problem (8) is said to be a complete smoothing dth degree spline. The space of complete smoothing dth degree splines is denoted by*

$$\mathcal{S}_{\mathrm{com},d}^{sm}\big(\Delta_n, S_L^i, S_R^i\big) = \{s_\rho\}_{\rho \geqslant 0}. \tag{11}$$

3. The generalized complete smoothing spline

Let us assume that

$$y_{n-1}/y_n > 1, \quad y_i \neq 0, \quad i = 1, \ldots, n. \tag{12}$$

We introduce the generalized smoothing spline that internally to the data interval Δ_n is a complete smoothing spline and outside the data interval, it mimics the Lt asymptotic behavior. The subsequent numerical analysis will address both the rational and the exponential asymptotic decay behavior. To this aim, in the following we refer to the rational decay and to the exponential decay by using the index $f \equiv r$ or $f \equiv e$, respectively, to define the function γ_f, where

$$\gamma_f(x, \text{pow}) = \begin{cases} x^{\text{pow}} & \text{if} \quad f \equiv r \\ \mathrm{e}^{x \cdot \text{pow}} & \text{if} \quad f \equiv e \end{cases} \tag{13}$$

and the function space

$$\mathcal{W}_f^g = \text{span}\{\gamma_f(x, -g)\} \qquad (x \in \text{Re}^+, \quad g \in \text{Re}). \tag{14}$$

Definition 3.1. *For $j = 2, \ldots, n$ let*[5]

$$\beta_j^f \cdot \gamma_f\left(x, -\alpha_j^f\right) \in \mathcal{W}_f^{\alpha_j^f}, \tag{15}$$

where

$$\alpha_j^f = \begin{cases} \dfrac{\ln(y_{j-1}/y_j)}{\ln(x_j/x_{j-1})}, & f \equiv r \\ \dfrac{\ln(y_{j-1}/y_j)}{x_j - x_{j-1}}, & f \equiv e \end{cases} \tag{16}$$

and

$$\beta_j^f = y_j \cdot \gamma_f\left(x_j, \alpha_j^f\right). \tag{17}$$

If $f \equiv r$, then the functions in (15) are referred to as the rational end behavior models (rational e.b.m); if $f \equiv e$, then these functions are referred to as the exponential end behavior models (exponential e.b.m).

Let us introduce Kronecker's symbol

$$\zeta_{a,b} = \begin{cases} 1 & a = b \\ 0 & a \neq b \end{cases}. \tag{18}$$

We assume $m = 2$, that is, we consider complete polynomial smoothing splines of degree $d = 3$[6]. Consider the regularization problem as defined in (8), where

$$\begin{aligned} S_L^1 &= \left[\beta_2^f \gamma_f\left(x_1, -\alpha_2^f\right)\right]^{(1)} = -\alpha_2^f y_1 \gamma_f(x_1, -\zeta_{f,r}) \\ S_R^1 &= \left[\beta_n^f \gamma_f\left(x_n, -\alpha_n^f\right)\right]^{(1)} = -\alpha_n^f y_n \gamma_f(x_n, -\zeta_{f,r}), \end{aligned} \tag{19}$$

whose solution is $s_\rho \in \mathcal{S}_{\text{com},3}^{sm}(\Delta_n, S_L^1, S_R^1)$, i.e. the complete smoothing spline of third degree.

Following [20], we introduce the space of generalized smoothing splines defined on $[x_1, +\infty)$ whose restriction in $[x_1, x_n]$ is a complete smoothing spline.

[5] The constants α_j^f and β_j^f will be obtained by requiring that each function in (15) interpolates the two points $P_{j-1} = (x_{j-1}, y_{j-1})$ and $P_j = (x_j, y_j)$.

[6] As explained by the sensitivity analysis in section 5, this choice gives the right trade-off between end regularity of the complete spline and conditioning of its numerical computation.

Definition 3.2. *Let $\mathcal{S}_{\mathcal{W}_f^g}$ be defined as follows:*

$$\mathcal{S}_{\mathcal{W}_f^g} = \left\{ \begin{array}{l} s_{\rho,g} : \text{ there exist } s_\rho \in \mathcal{S}^{sm}_{\text{com},3}(\Delta_n, S_L^1, S_R^1),\, s_g \in \mathcal{W}_f^g : \\ s_{\rho,g} \equiv s_\rho \text{ on } [x_1, x_n],\, s_{\rho,g} \equiv s_g \text{ on } [x_n, \infty) \text{ and} \\ s_\rho(x_n) = s_g(x_n),\, s_\rho^{(1)}(x_n) = s_g^{(1)}(x_n) \end{array} \right\}.$$

If the index f equals r, then the function $s_{\rho,g} \in \mathcal{S}_{\mathcal{W}_f^g}$ is said to be a generalized complete smoothing spline with rational end behavior; if the index f equals e, then it is said to be a generalized complete smoothing spline with exponential end behavior.

The next result addresses the existence and uniqueness of the generalized complete smoothing spline.

Theorem 3.3. *Let s_ρ be the solution of (8), where $\rho \geqslant 0$. Let*

$$\alpha_n^f(\rho) = \begin{cases} -x_n s_\rho^{(1)}(x_n)/s_\rho(x_n) & \text{if } f \equiv r\,, \\ -s_\rho^{(1)}(x_n)/s_\rho(x_n) & \text{if } f \equiv e \end{cases} \tag{20}$$

and

$$\beta_n^f(\rho) = s_\rho(x_n)\gamma_f(x_n, \alpha_n^f(\rho)). \tag{21}$$

For every $\rho \geqslant 0$, there exists a unique $s_{\rho,\alpha_n^f(\rho)} \in \mathcal{S}_{\mathcal{W}_f^{\alpha_n^f(\rho)}}$, whose restriction on $[x_1, x_n]$ is s_ρ, and whose restriction on $[x_n, \infty)$ is $s_{\alpha_n^f(\rho)}(x) = \beta_n^f(\rho)\gamma_f(x, -\alpha_n^f(\rho)) \in \mathcal{W}_f^{\alpha_n^f(\rho)}$.

As $\rho \to \infty$, the function $s_{\alpha_n^f(\rho)}$ converges to the polynomial of degree $m-1$ which fits data $(x_i, y_i)_{i=1,\ldots,n}$ best in the least-squares sense.

Moreover, if $\rho = 0$, then s_0 is the dth degree complete spline interpolating $(x_i, y_i)_{i=1,\ldots,n}, S_L^1, S_R^1$. $\alpha_n^f(\rho)$ and $\beta_n^f(\rho)$ become α_n^f and β_n^f as defined in (16), (17) and $s_{\alpha_n^f(\rho)}$ is $s_{\alpha_n^f}(x) = \beta_n^f \gamma_f(x, -\alpha_n^f)$.

Proof. $s_{\rho,\alpha_n^f(\rho)} \in \mathcal{S}_{\mathcal{W}_f^{\alpha_n^f(\rho)}}$ is obtained from $s_\rho \in \mathcal{S}^{sm}_{\text{com},3}(\Delta_n, S_L^1, S_R^1)$ on $[x_1, x_n)$ and from $\beta_n^f(\rho)\gamma_f(x, -\alpha_n^f(\rho))$ on $[x_n, \infty)$. Existence and uniqueness of s_ρ at $[x_1, x_n)$ are derived from theorem 2.4. Moreover, if continuity conditions in x_n of the function $s_{\rho,\alpha_n^f(\rho)}$ imply

$$s_{\alpha_n^f(\rho)}(x_n) = \beta_n^f(\rho)\gamma(x_n, -\alpha_n^f(\rho)) = s_\rho(x_n), \quad s^{(1)}_{\alpha_n^f(\rho)}(x_n) = s_\rho^{(1)}(x_n),$$

then $s_{\rho,\alpha_n^f(\rho)}$ on $[x_n, \infty)$ coincides with the end behavior model defined by (20) and (21).

As $\rho \to \infty$, from theorem 2.4, the function $s_{\alpha_n^f(\rho)}$ converges to the polynomial of degree $m-1$ which fits data $(x_i, y_i)_{i=1,\ldots,n}$ best in the least-squares sense. From theorem 2.4, as $\rho \to 0$, $s_{\alpha_n^f(0)}$ is the dth degree complete spline interpolating $(x_i, y_i)_{i=1,\ldots,n}, S_L^1, S_R^1$. Finally, if $\rho = 0$, then from (20) it is

$$\alpha_n^f(0) = \frac{-\gamma_f(x_n, \zeta_{f,r}) s_0^{(1)}(x_n)}{s_0(x_n)}$$

and from (5) it is

$$\frac{-\gamma_f(x_n, \zeta_{f,r}) S_R^1}{y_n}$$

which, from (18), is equal to α_n^f. By the same way, from (21) we obtain

$$\beta_n^f(0) = s_0(x_n)\gamma_f(x_n, \alpha_n^f(0))$$

which from (17) is equal to β_n^f. □

4. Error analysis

We consider the interpolating generalized complete spline $s_{\alpha_n^f(0)}$, with rational (if $f \equiv r$) or exponential (if $f \equiv e$) end behavior, obtained by setting $\rho = 0$ in theorem 3.3. For the sake of simplicity, we denote this function by s_F.

Moreover, we set

$$y_j^{(k)} = F^{(k)}(x_j), \quad j = 1, \ldots, n \quad , k \geqslant 0, \tag{22}$$

$$\begin{aligned} &h_{j+1} = x_{j+1} - x_j, \quad j = 1, \ldots, n-1, \\ &\|\Delta_n\| = \max_{j=2,\ldots,n} h_j, \\ &h_{\min} = \min(h_2, h_n). \end{aligned} \tag{23}$$

Definition 4.1. *We define*

$$E_j(x) = E_j(F, [x_j, x_{j+1})) = \max_{x \in [x_j, x_{j+1})} |s_F(x) - F(x)|, \qquad j = 1, \ldots, n, \tag{24}$$

to be the error at $[x_j, x_{j+1})$*, measuring the distance between* F *and* s_F*.*

The main result of this section is to provide computable estimates of the errors E_j for $j = 1, \ldots, n$. To this aim, we first determine upper bounds of E_j (see theorem 4.2 in the case of $j = n$, and theorem 4.7, if $j < n$), and then we replace these upper bounds with computable quantities (see theorem 4.5 in the case of $j = n$ and theorem 4.8, if $j < n$), i.e. with quantities that can be obtained only using data points. Finally, we give the definition of computable estimates of E_j (see definition 4.6 if $j = n$ and definition 4.9, if $j < n$).

Let us consider $E_n(x)$ for $x \geqslant x_n$. Then the following result holds.

Theorem 4.2. *If we set*

$$B_n = |D_n^f| \frac{|a_1|}{\gamma_f(x_n, \alpha)} + \max \left\{ |D_n^f| \frac{|a_1|}{\gamma_f(x_n, \alpha)} \, , \, \frac{|\alpha_n^f - \alpha|}{\alpha} |y_n| \right\}, \tag{25}$$

where

$$D_j^f = \frac{a_2}{a_1 \, \gamma_f(x_j, \delta)}, \quad j = 1, \ldots, n, \tag{26}$$

and the Lt function $F \in \mathcal{R}^{\alpha}_{\text{decay}}$ *is as in (3), if* $f \equiv r$*, or* $F(x) \equiv F_1(x) \in \mathcal{E}^{\alpha}_{\text{decay}}$*, where* $F_1(x) = a_1 \mathrm{e}^{-\alpha x} + a_2 \mathrm{e}^{-(\alpha+\delta)x} + o\left(\mathrm{e}^{-(\alpha+\delta)x}\right)$*, if* $f \equiv e$*,* α_n^f *and* β_n^f *are as in (16) and (17), and* $s_F \in \mathcal{S}_{\mathcal{W}_f^g}$*, it holds that*

$$E_n(x) \leqslant B_n \quad (x \geqslant x_n).$$

In order to prove this result we need the following two lemmas.

Lemma 4.3. *In the same hypothesis of theorem 4.2, let*

$$\psi(x) = \left| \frac{a_1}{\gamma_f(x, \alpha)} - \frac{\beta_n^f}{\gamma(x, \alpha_n^f)} \right|$$

and $x \geqslant x_n$*. If*

$$\alpha_n^f = \alpha \quad \text{or } \beta_n^f / a_1 < 0, \tag{27}$$

then ψ *is a decreasing function on* $[x_n, \infty)$*.*

Proof. If $\alpha_n^f = \alpha$, from (17), we have that

$$\psi(x) = \left| \frac{a_1}{\gamma_f(x,\alpha)} - y_n \frac{\gamma_f(x_n,\alpha_n^f)}{\gamma_f(x,\alpha_n^f)} \right| = \left| \frac{1}{\gamma_f(x,\alpha)} [a_1 - \gamma_f(x_n,\alpha)] \right|$$

which is a decreasing function with respect to x because it is the product of a constant term with $|\frac{1}{\gamma_f(x,\alpha)}|$ which is a decreasing function with respect to x.

Let $M = -\beta_n^f/a_1$; if $M > 0$, then

$$\psi(x) = \left| \frac{a_1}{\gamma_f(x,\alpha)} - \frac{\beta_n^f}{\gamma_f(x,\alpha_n^f)} \right| = \left| a_1 \left(\frac{1}{\gamma_f(x,\alpha)} + \frac{M}{\gamma_f(x,\alpha_n^f)} \right) \right|$$

is a decreasing function of x because it is the sum of two decreasing functions of x. □

Lemma 4.4. *In the same hypothesis of theorem 4.2, let $\psi(x)$ be defined as in lemma 4.3. Then*

$$\max_{x \geqslant x_n} \psi(x) \leqslant \max \left\{ \frac{|a_2|}{\gamma_f(x_n,\alpha+\delta)}, \frac{|\alpha_n^f - \alpha|}{\alpha} |y_n| \right\}.$$

Proof. We consider two cases.

(i) If

$$\beta_n^f/a_1 < 0 \quad or \quad \alpha_n^f = \alpha, \tag{28}$$

then from lemma 4.3 ψ is a decreasing function on $[x_n, \infty)$. Hence, $\psi(x_n)$ is the global maximum of $\psi(x)$. From (16) and (17) it follows

$$\psi(x_n) = \left| \frac{a_1}{\gamma_f(x_n,\alpha)} - \frac{\beta_n^f}{\gamma_f(x_n,\alpha_n^f)} \right| = \left| \frac{a_1}{\gamma_f(x_n,\alpha)} - y_n \right| \leqslant \frac{|a_2|}{\gamma_f(x_n,\alpha+\delta)},$$

where the last inequality is true taking into account the hypothesis on F. In the first case the thesis follows.

(ii) If (28) is not verified, then a unique local maximum of ψ is at $\bar{x} = \left(\frac{\alpha_n^f \beta_n^f}{a_1 \alpha}\right)^{\frac{1}{\alpha_n^f - \alpha}}$ if $f \equiv r$ or $\bar{x} = \ln\left(\frac{\alpha_n^f \beta_n^f}{a_1 \alpha}\right)^{\frac{1}{\alpha_n^f - \alpha}}$ if $f \equiv e$. We obtain

$$\psi(\bar{x}) = \left| a_1 \gamma_f(\bar{x}, -\alpha) - \beta_n^f \gamma_f(\bar{x}, -\alpha_n^f) \right| = \left| \frac{a_1 \gamma_f(\bar{x}, \alpha_n^f - \alpha) - \beta_n^f}{\gamma_f(\bar{x}, \alpha_n^f)} \right| = \left| \frac{a_1 \frac{\alpha_n^f \beta_n^f}{a_1 \alpha} - \beta_n^f}{\gamma_f(\bar{x}, \alpha_n^f)} \right|$$

$$\leqslant \left| \frac{\alpha_n^f - \alpha}{\alpha} \frac{\beta_n^f}{\gamma_f(\bar{x}, \alpha_n^f)} \right| \leqslant \frac{|\alpha_n^f - \alpha|}{\alpha} |y_n|.$$

□

Let us demonstrate theorem 4.2.

Proof. By adding and subtracting $a_1/\gamma_f(x,\alpha)$ to $s_F(x) - F(x)$ and taking into account that for $x \geqslant x_n$, s_F is the end behavior model (15), we obtain

$$E_n = \max_{x \geqslant x_n} \left| s_F(x) - F(x) - a_1/\gamma_f(x,\alpha) + a_1/\gamma_f(x,\alpha) \right|$$

$$\leqslant \max_{x \geqslant x_n} \left| F(x) - \frac{a_1}{\gamma_f(x,\alpha)} \right| + \max_{x \geqslant x_n} \left| \frac{a_1}{\gamma_f(x,\alpha)} - \frac{\beta_n^f}{\gamma_f(x,\alpha_n^f)} \right|.$$

For the first addend, taking the hypothesis on F it follows that

$$\max_{x\geqslant x_n}\left|F(x)-\frac{a_1}{\gamma_f(x,\alpha)}\right|=\max_{x\geqslant x_n}\left|\frac{a_2}{\gamma_f(x,\alpha+\delta)}+o\left(\frac{1}{\gamma_f(x,\alpha+\delta)}\right)\right|$$
$$\leqslant\frac{|a_2|}{\gamma_f(x_n,\alpha+\delta)}. \tag{29}$$

For the second addend, using lemma 4.4, we obtain

$$\max_{x\geqslant x_n}\left|\frac{a_1}{\gamma_f(x,\alpha)}-\frac{\beta_n^f}{\gamma_f(x,\alpha_n^f)}\right|\leqslant\max\left\{\frac{|a_2|}{\gamma_f(x_n,\alpha+\delta)},\frac{|\alpha_n^f-\alpha|}{\alpha}|y_n|\right\}. \tag{30}$$

Collecting (29) and (30), it follows that

$$E_n\leqslant\frac{|a_2|}{\gamma_f(x_n,\alpha+\delta)}+\max\left\{\frac{|a_2|}{\gamma_f(x_n,\alpha+\delta)},\frac{|\alpha_n^f-\alpha|}{\alpha}|y_n|\right\}$$

and the thesis follows. □

Theorem 4.2 provides an upper bound of the error E_n. Unfortunately, B_n depends on quantities that are not known *a priori*; hence, E_n may not be estimated only using data. Our aim is to get to an approximation of B_n, and thus of E_n, which is actually computable, i.e. only using data. In this way, we are able to provide the estimate of the approximation error introduced by replacing the function F by the generalized smoothing spline s_F. This estimate may be useful, for instance, to validate the solution computed by any Lt inversion algorithm.

Corollary 4.5. *In the same hypothesis of theorem 4.2, an approximation of B_n is given by*

$$|y_n||D_n^f|+\max\left\{|y_n||D_n^f|\,,\ \frac{|\alpha_n^f-\alpha|}{\alpha_n^f}|y_n|\right\}. \tag{31}$$

Proof. It follows by taking into account that in (25) $y_n=F(x_n)=a_1/\gamma_f(x_n,\alpha)$. □

The following proposition provides an approximation of $|\alpha_n^f-\alpha|$.

Proposition 4.6. *If α_j^f is defined as in (16), then for $j=2,\ldots,n$ it is*

$$\alpha_j^f=\alpha+\delta D_j^f+\mathcal{O}(h_j). \tag{32}$$

Proof. From Taylor's formula of the $\ln(1+z)$ function centered at zero,

$$\ln(1+z)=z-z^2/2+o(z^2)\,,\quad (z\to 0), \tag{33}$$

using $1+z=\frac{y_{j-1}}{y_j}$ in (33), we obtain

$$\ln\frac{y_{j-1}}{y_j}=\left(\frac{y_{j-1}}{y_j}-1\right)-\frac{1}{2}\left(\frac{y_{j-1}}{y_j}-1\right)^2+o\left(\left(\frac{y_{j-1}-y_j}{y_j}\right)^2\right).$$

Taking into account that if $h_j\to 0$, then $y_{j-1}\to y_j$, we may write that

$$\ln\frac{y_{j-1}}{y_j}=\left(\frac{y_{j-1}}{y_j}-1\right)-\frac{1}{2}\left(\frac{y_{j-1}}{y_j}-1\right)^2+o\left(h_j^2\right).$$

Taking Taylor's formula of F centered at x_j evaluated at x_{j-1},

$$F(x_{j-1})=F(x_j)-h_jF^{(1)}(x_j)+\tfrac{1}{2}h_j^2(F^{(2)}(x_j))^2+o\big(h_j^2\big)$$

and using the relations in (22), we obtain

$$y_{j-1}=F(x_{j-1})=y_j-h_jy_j^{(1)}+\tfrac{1}{2}h_j^2(y_j^{(2)})^2+o\big(h_j^2\big). \tag{34}$$

Hence, it follows

$$\ln\frac{y_{j-1}}{y_j} = \frac{-h_j y_j^{(1)} + h_j^2/2\big(y_j^{(2)}\big)^2 + o\big(h_j^2\big)}{y_j} - \frac{1}{2}\left(\frac{h_j y_j^{(1)} + h_j^2/2\big(y_j^{(2)}\big)^2 + o\big(h_j^2\big)}{y_j}\right)^2 + o\big(h_j^2\big)$$

$$= -\frac{h_j y_j^{(1)}}{y_j} + \frac{h_j^2 (y_j^{(2)})^2}{2y_j} - \frac{1}{2}\left(\frac{h_j y_j^{(1)}}{y_j}\right)^2 + o\big(h_j^2\big)$$

$$= h_j\left[-\frac{y_j^{(1)}}{y_j} + \frac{h_j}{2}\frac{(y_j^{(2)})^2}{y_j} - \frac{h_j}{2}\left(\frac{y_j^{(1)}}{y_j}\right)^2 + o(h_j)\right].$$

Finally, we obtain

$$\frac{1}{h_j}\ln\frac{y_{j-1}}{y_j} = -\frac{y_j^{(1)}}{y_j} - \frac{h_j}{2}\left[\left(\frac{y_j^{(1)}}{y_j}\right)^2 + \frac{\big(y_j^{(2)}\big)^2}{y_j} + o(h_j)\right]. \tag{35}$$

By using the properties of the ln function, it follows that

$$\left(\ln\frac{x_j}{x_{j-1}}\right)^{-1} = \left(-\ln\left(\frac{x_{j-1}}{x_j}\right)\right)^{-1} = -\left(\ln\left(1-\frac{h_j}{x_j}\right)\right)^{-1} = -\frac{1}{\ln\left(1-\frac{h_j}{x_j}\right)},$$

that is, by using (33), where $z = -\frac{h_j}{x_j}$,

$$\left(\ln\frac{x_j}{x_{j-1}}\right)^{-1} = -\frac{1}{-\frac{h_j}{x_j} - 1/2(\frac{h_j}{x_j})^2 + o\big(h_j^2\big)} = \frac{1}{\frac{h_j}{x_j} + 1/2(\frac{h_j}{x_j})^2 + o\big(h_j^2\big)}$$

$$= \frac{x_j}{h_j}\left(\frac{1}{1+1/2\frac{h_j}{x_j} + \mathcal{O}\big(h_j^2\big)}\right) = \frac{x_j}{h_j}\left(1 - \frac{1}{2}\frac{h_j}{x_j} + \mathcal{O}\big(h_j^2\big)\right). \tag{36}$$

By multiplying (35) and (36), we have

$$\frac{\ln\frac{y_{j-1}}{y_j}}{\ln\frac{x_j}{x_{j-1}}} = -x_j\left[\frac{y_j^{(1)}}{y_j} + \frac{h_j}{2}\left(\left(\frac{y_j^{(1)}}{y_j}\right)^2 + \frac{\big(y_j^{(2)}\big)^2}{y_j}\right) - \frac{h_j}{2x_j}\frac{y_j^{(1)}}{y_j}\right] + \mathcal{O}(h_j);$$

then

$$\alpha_j^e = \frac{1}{h_j}\ln\frac{y_{j-1}}{y_j} = -\frac{y_j^{(1)}}{y_j} + \frac{h_j}{2}\left(\left(\frac{y_j^{(1)}}{y_j}\right)^2 + \frac{\big(y_j^{(2)}\big)^2}{y_j}\right) + \mathcal{O}(h_j)$$

and

$$\alpha_j^r = \frac{\ln\frac{y_{j-1}}{y_j}}{\ln\frac{x_j}{x_{j-1}}} = -x_j\left[\frac{y_j^{(1)}}{y_j} - \frac{h_j}{2}\left(\left(\frac{y_j^{(1)}}{y_j}\right)^2 + \frac{\big(y_j^{(2)}\big)^2}{y_j}\right) - \frac{h_j}{2x_j}\frac{y_j^{(1)}}{y_j}\right] + \mathcal{O}(h_j).$$

These relations can be rewritten as

$$\alpha_j^e = -\frac{y_j^{(1)}}{y_j} + \mathcal{O}(h_j)$$

and

$$\alpha_j^r = -x_j\frac{y_j^{(1)}}{y_j} + \mathcal{O}(h_j).$$

If $F \in \mathcal{R}^{\alpha}_{\text{decay}}$ as in (3), then for $x \geqslant x_n$ we obtain

$$-\frac{y_j^{(1)} x_j}{y_j} = \frac{\left[\alpha \frac{a_1}{x_j^{\alpha+1}} + (\alpha+\delta)\frac{a_2}{x_j^{\alpha+\delta+1}}\right] x_j}{F(x_j)} = \frac{\alpha F(x_j) + \delta \frac{a_2}{x_j^{\alpha+\delta}}}{F(x_j)} = \alpha + \delta \frac{a_2}{a_1}\frac{1}{x_j^{\delta}} = \alpha + \delta D_j^r.$$

If $F \equiv F_1(x) \in \mathcal{E}^{\alpha}_{\text{decay}}(\Omega))$, as in theorem 4.2, then we obtain

$$-\frac{y_j^{(1)}}{y_j} = \frac{\alpha \frac{a_1}{\mathrm{e}^{\delta x_j}} + (\alpha+\delta)\frac{a_2}{\mathrm{e}^{(\alpha+\delta)x_j}}}{F(x_j)}$$

$$= \frac{\alpha F(x_j) + \delta \frac{a_2}{\mathrm{e}^{(\alpha+\delta)x_j}}}{F(x_j)} = \alpha + \delta \frac{a_2}{a_1}\frac{1}{\mathrm{e}^{\delta x_j}} = \alpha + \delta D_j^e.$$

By collecting these results it follows that

$$\alpha_j^f = \alpha + \delta D_j^f + \mathcal{O}(h_j).$$

□

The following proposition provides a computable expression of D_j^f.

Proposition 4.7. *Let*

$$\overline{D}_j^{\,f} = \gamma_f(x_{j-1}, \zeta_{f,r}) \frac{\alpha_j^f - \alpha_{j-1}^f}{x_j - x_{j-1}}, \tag{37}$$

where $\zeta_{f,r}$ is defined as in (18), be computed at $j = 2, \ldots, n$. It follows that

$$|\overline{D}_j^{\,f}| \quad \geqslant \quad |D_j^f| + \mathcal{O}(h_j).$$

Proof. By definition of $\overline{D}_j^{\,f}$, if $f \equiv r$, then it follows that

$$\overline{D}_j^{\,r} = x_{j-1} \frac{\alpha_j^r - \alpha_{j-1}^r}{x_j - x_{j-1}} \tag{38}$$

while, if $f \equiv e$,

$$\overline{D}_j^{\,e} = \frac{\alpha_j^e - \alpha_{j-1}^e}{x_j - x_{j-1}}. \tag{39}$$

If $f \equiv r$, from (32), we obtain

$$\overline{D}_j^{\,r} = x_{j-1}\delta \frac{D_j^r - D_{j-1}^r}{h_j} + \mathcal{O}(h_j) = x_{j-1}\delta \frac{1 - \frac{x_j^{\delta}}{x_{j-1}^{\delta}}}{h_j} D_j^r + \mathcal{O}(h_j)$$

$$= x_{j-1}\delta \frac{1 - \left(1 + \frac{h_j}{x_{j-1}}\right)^{\delta}}{h_j} D_j^r + \mathcal{O}(h_j) = -\delta^2 D_j^r + \mathcal{O}(h_j),$$

while, if $f \equiv e$, it holds that

$$\overline{D}_j^{\,e} = \delta \frac{D_j^e - D_{j-1}^e}{h_j} + \mathcal{O}(h_j) \tag{40}$$

$$= \delta \frac{1 - \frac{D_{j-1}^e}{D_j^e}}{h_j} D_j^e + \mathcal{O}(h_j) = \delta \frac{1 - \mathrm{e}^{\delta h_j}}{h_j} D_j^e + \mathcal{O}(h_j)$$

$$= -\delta^2 D_j^e + \mathcal{O}(h_j). \tag{41}$$

By assuming $\delta \geqslant 1$, it follows that

$$|\overline{D}_j^{\,r}| \geqslant \delta |D_j^r| + \mathcal{O}(h_j) \geqslant |D_j^r| + \mathcal{O}(h_j) \tag{42}$$

and

$$\left|\overline{D}_j^{\,e}\right| \geqslant \delta |D_j^e| + \mathcal{O}(h_j) \geqslant |D_j^e| + \mathcal{O}(h_j). \tag{43}$$

Collecting (42) and (43), by assuming $\delta \geqslant 1$, it follows that

$$|\overline{D}_j^{\,f}| \quad \geqslant \delta |D_j^f| + \mathcal{O}(h_j) \geqslant |D_j^f| + \mathcal{O}(h_j).$$

□

Finally, we may give the following definition.

Definition 4.8. *Let*

$$\overline{B}_n = \left|y_n\, \overline{D}_n^f\right| + \max\left\{\left|y_n\, \overline{D}_n^f\right|, \frac{\left|y_n\, \overline{D}_n^f\right|}{\alpha_n}\right\}$$

be the computable estimate of E_n.

The restriction of s_F at $[x_1, x_n]$ is the complete third degree spline interpolating $(x_i, z_i)_{i=1,\ldots,n}$, S_L^1, S_R^1 as defined in 2.3, then, if

$$|F^{(4)}(x)| \leqslant L_j, \quad x \in I_j = [x_j, x_{j+1}], \quad \text{for} \quad j = 1, \ldots, n-1,$$

we make use of the following result.

Theorem 4.9 [24]**.** *Let* $F \in C^4[x_1, x_n]$ *and* $s_F \in \mathcal{S}_{\mathcal{W}_f^{\alpha_n^f}}$ *then, if*

$$B_j = h_{j+1}^2 \cdot R(\|\Delta_n\|^2) + \frac{h_{j+1}^4}{4} L_j = \mathcal{O}(\|\Delta_n\|^4), \tag{44}$$

where $R(\|\Delta_n\|^2) = \max_{j=1,\ldots,n} r_j$ *and*

$$\begin{aligned} r_1 &= \frac{3}{4} h_2^2 L_1, \\ r_j &= \frac{3}{4} \max(h_j, h_{j+1})^2 \max(L_j, L_{j+1}) \quad (j = 2, \ldots, n-1), \\ r_n &= \frac{3}{4} h_n^2 L_{n-1}, \end{aligned} \tag{45}$$

then it holds

$$E_j \leqslant B_j, \qquad j = 1, \ldots, n-1.$$

Theorem 4.10. *If* $F \in \mathcal{R}^{\alpha}_{\text{decay}}(\Omega)$ *(or* $F \equiv F_1(x) \in \mathcal{E}^{\alpha}_{\text{decay}}(\Omega)$*, where* $F_1(x) = a_1 \mathrm{e}^{-\alpha x} + a_2 \mathrm{e}^{-(\alpha+\delta)x} + o(\mathrm{e}^{-(\alpha+\delta)x})$*)* $F \in C^4[x_1, x_n]$ *and* $s_F \in \mathcal{S}_{\mathcal{W}_f^{\alpha_n^f}}$*, then,*

$$\overline{L}_j^f = \frac{\left(\alpha_{j+1}^f\right)^{(4)_f}}{\gamma_f(x_j, 4 \cdot \zeta_{f,r})} |y_j| \tag{46}$$

where

$$(4)_f = \begin{cases} (4) & f \equiv r \\ 4 & f \equiv e, \end{cases}$$

while (4) *indicates the exponential of a rising factorial*[7] *and* $\zeta_{a,b}$ *is the Kronecker symbol defined in (18). If* $x \to \infty$, *it holds that*

$$L_j = \overline{L}_j^{\,f} + o\left(\frac{1}{\gamma_f(x, \alpha + 4 \cdot \zeta_{f,r})}\right).$$

Proof. If $F \in \mathcal{R}^{\alpha}_{\text{decay}}(\Omega)$, then from (3) we obtain

$$|L_j| = \max_{I_j} |F^{(4)}| = \max_{I_j} \left| \frac{\alpha^{(4)} a_1}{x^{\alpha+4}} + o\left(\frac{1}{x^{\alpha+4}}\right) \right|.$$

By replacing F by the function in (15), it follows

$$|L_j| = \left| \frac{\left(\alpha^r_{j+1}\right)^{(4)} \beta^r_{j+1}}{x_j^{\alpha^r_{j+1}+4}} \right| + o\left(\frac{1}{x^{\alpha+4}}\right) = \frac{\left(\alpha^r_{j+1}\right)^{(4)}}{x_j^4} \left|y_j\right| + o\left(\frac{1}{x^{\alpha+4}}\right), \tag{47}$$

where $\alpha^{(4)}$ and $\left(\alpha^r_j\right)^{(4)}$ are rising factorials. By setting in (47)

$$\overline{L}^r_j = \frac{\left(\alpha^r_{j+1}\right)^{(4)}}{x_j^4} |y_j|, \tag{48}$$

it follows that

$$|L_j| = \overline{L}_j^{\,r} + o\left(\frac{1}{x^{\alpha+4}}\right).$$

If $F \in \mathcal{E}^{\alpha}_{\text{decay}}(\Omega)$, then we obtain

$$|L_j| = \max_{I_j} |F^{(4)}| = \max_{I_j} \left| \frac{\alpha^4 a_1}{\mathrm{e}^{\alpha x}} + o\left(\frac{1}{\mathrm{e}^{\alpha x}}\right) \right|.$$

By replacing F by the function in (15), it follows that

$$|L_j| = \left| \frac{\left(\alpha^e_{j+1}\right)^4 \beta^e_{j+1}}{\mathrm{e}^{\alpha^e_{j+1} x}} \right| + o\left(\frac{1}{\mathrm{e}^{\alpha x}}\right) = \left(\alpha^e_{j+1}\right)^4 \left|y_j\right| + o\left(\frac{1}{\mathrm{e}^{\alpha x}}\right). \tag{49}$$

By setting in (49)

$$\overline{L}^e_j = (\alpha^e_{j+1})^4 |y_j|, \tag{50}$$

it follows that

$$|L_j| = \overline{L}^e_j + o\left(\frac{1}{\mathrm{e}^{\alpha x}}\right).$$

By collecting these results, we obtain

$$|L_j| = \frac{\left(\alpha^r_{j+1}\right)^{(4)_f}}{\gamma_f(x_j, 4 \cdot \zeta_{f,r}))} \left|y_j\right| + o\left(\frac{1}{\gamma_f(x, \alpha + 4 \cdot \xi_{f,r})}\right). \tag{51}$$

Hence, the thesis follows. □

As expected, a sharper bound of E_j can be obtained by substituting $R(\|\Delta_n\|^2)$ in (44) by r_j in (45). Hence, we give the following.

[7] The rising factorial is defined as

$$x^{(n)} = x(x+1)(x+2)\cdots(x+n-1).$$

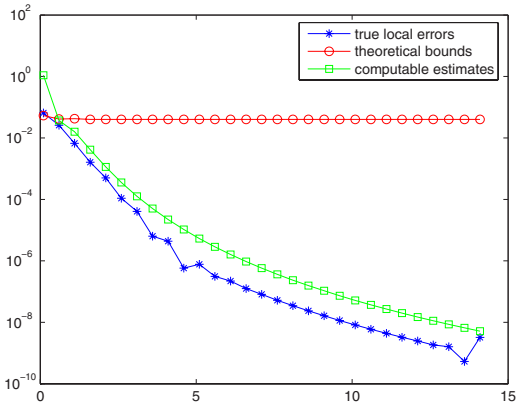

Figure 1. Experiment 1: local errors E_j ($-*$) versus theoretical bounds B_j ($-$o) versus computable estimates $\overline{B}_j$ ($-\square$). x-values belong to the sample interval [0.1,14.6].

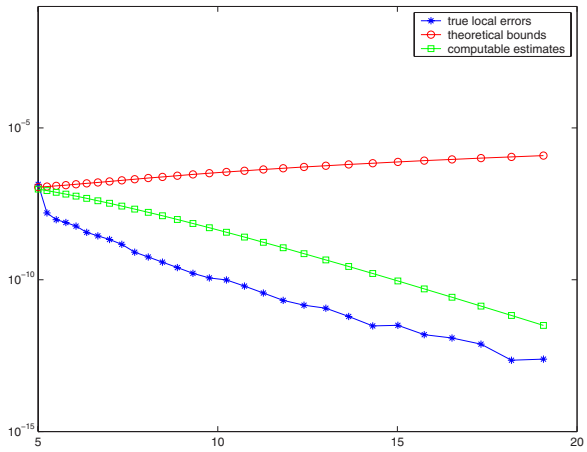

Figure 2. Experiment 2: local errors E_j ($-*$) versus theoretical bounds B_j ($-$o) versus computable estimates $\overline{B}_j$ ($-\square$). x-values belong to the sample interval [19].

Definition 4.11. *If*

$$\overline{r}_1 = \tfrac{3}{4}h_2^2\overline{L}_1^f, \quad \overline{r}_j = \tfrac{3}{4}\max\left(h_j, h_{j+1}\right)^2 \max(\overline{L}_j^f, \overline{L}_{j+1}^f), \quad \overline{r}_{n-1} = \tfrac{3}{4}h_n^2\overline{L}_{n-1}^f,$$

then

$$\overline{B}_j = h_{j+1}^2\overline{r}_j + \frac{h_{j+1}^4}{4}\overline{L}_j^f \tag{52}$$

is the computable estimate of $E_j \quad (j = 1, \ldots, n-1)$.

In figures 1 and 2, we show the behavior of E_j compared with its theoretical bound B_j and the computable estimate $\overline{B}_j$ for a Lt $F \in \mathcal{R}^{\alpha}_{\text{decay}}$ (experiment 1) and for a Lt $F \in \mathcal{E}^{\alpha}_{\text{decay}}$ (experiment 2), respectively. Following [1], we consider two data point distributions: uniform and geometric; the former is characterized by giving the distance between two adjacent points, and the latter by giving the ratio between two adjacent points. Geometrical sampling is a

uniform sampling in the variable $\ln(x)$ and this is the reason why it seems to be natural for the Lt. We consider these distributions because the Lt function may be uniquely determined by them as the number of points tends to infinity.

Experiment 1. *Generalized complete smoothing spline with rational end behavior.* Assume that

$$F(x) = 2x/((1+x^2)^2)$$

is only known at $n = 30$ real samples $\Delta_n = \{x_1 = 0.1, \ldots, x_n = 14.6\}$ linearly equi-spaced between x_1 and x_n. If $F \in \mathcal{R}^3_{\text{decay}}(\text{Re})$, we obtain $\overline{B}_n = 5.08 \times 10^{-5}$ and $E_n = 5.42 \times 10^{-7}$. Observe that $F(x_n) = 6.36 \times 10^{-4}$, i.e. the generalized complete smoothing spline s_F with rational end behavior offers a sharp approximation of the asymptotic behavior of F.

Experiment 2. *Generalized complete smoothing spline with exponential end behavior.* Assume that

$$F(x) = \mathrm{e}^{-x}(x+1)^{-1}$$

is only known at $n = 30$ real samples $\Delta_n = \{x_1 = 5, \ldots, x_n = 20\}$ distributed between x_1 and x_n as follows:

$$x_1 = a, \qquad x_n = b, \qquad x_{i+1} = x_i \cdot (b/a)^{1/(n-1)}, \quad i = 1, ..., n-1.$$

If $F \in \mathcal{E}^{\alpha}_{\text{decay}}(\Omega)$, we obtain $\overline{B}_n = 9.07 \times 10^{-12}$ and $E_n = 8.30 \times 10^{-14}$. Observe that $F(x_n) = 9.8150 \times 10^{-11}$, i.e. the generalized complete smoothing spline s_F with exponential end behavior offers a sharp approximation of the asymptotic behavior of F.

5. Sensitivity analysis

This section analyzes the round-off error propagation on $s(x)$ where $x \in [x_1, \infty)$ and $s = s_{\rho,\alpha^f_n(\rho)}$ is the generalized complete smoothing spline of degree $d = 2m-1$, $m > 0$. Let us introduce the following application $\mathcal{P}$:

$$\mathcal{P} : ((x_1, y_1), \ldots, (x_n, y_n), x) \in \left(\text{Re}^2\right)^n \times \text{Re} \mapsto s(x) \in \text{Re}. \tag{53}$$

We write $\mathcal{P}$ as $\mathcal{P} = \mathcal{P}_2 \circ \mathcal{P}_1$, where

(i) $\mathcal{P}_1$ describes the computation of s and
(ii) $\mathcal{P}_2$ describes the evaluation of s.

Consider the representation of s as a linear combination of B-splines as given in [4]:

$$s(x) = \sum_{j=1}^{n+2m-2} c_j N_j^{2m}(x), \tag{54}$$

where N_j^{2m} is the normalized B-spline of order $2m$ on $[\tau_j, \tau_{j+2m}]$ and

$$\tau_i = x_1, \ \tau_{n+2m-2+i} = x_n, \quad i = 1, \ldots, 2m, \quad \text{and} \quad \tau_{2m+i-1} = x_i, \ i = 2, \ldots, n-1.$$

c is the solution of the linear system [4]

$$(B + \rho E)c = z, \tag{55}$$

where

$$z = (S_L^{m-1}, \ldots, S_L^1, y_1, \ldots, y_n, S_R^1, \ldots, S_R^{2m-1})^t, \tag{56}$$

and for $j = 1, \ldots, n+2m-2$:

$$B_{ij} = \begin{cases} D^{m-i}N_j^{2m}(x_1) & i = 1, \ldots, m \\ N_j^{2m}(x_{i-m+1}) & i = m+1, \ldots, m+n-2 \\ D^{i-m-n+1}N_j^{2m}(x_n) & i = m+n-1, \ldots, n+2m-2 \end{cases}$$

and

$$E_{ij} = \begin{cases} (-1)^i (w^L_{m-i})^{-1} D^{m+i-1} N^{2m}_j(x_1) & i = 1, \ldots, m-1 \\ (-1)^m (w_{i-m+1})^{-1} D^{2m-1} N^{2m}_j(x_{i-m+1}) & i = m, \ldots, m+n-1 \\ (-1)^{n+2m-2-i} (w^R_{i-m-n+1})^{-1} D^{n+3m-2-i} N^{2m}_j(x_n) & i = m+n, \ldots, n+2m-2. \end{cases}$$

So we obtain

(i) $\mathcal{P}_1$: given (x_i, y_i), computes the coefficients c solving the linear system (55);
(ii) $\mathcal{P}_2$: given c and x, evaluates (54).

In the following, we analyze the round-off error propagation of steps (i) and (ii). The main results of this section are theorem 5.4 (for step (i)) and theorem 5.5 (for step (ii)). We show that, if the linear system (55) is well conditioned, then the round-off error propagates linearly as θ, the initial error on y_i, depending on the reciprocal of $h_{\min} = \min(h_2, h_n)$. Furthermore, for $x \geqslant x_n$, the distance between $s(x)$ and $s_\theta(x)$ grows linearly as θ depending on $|y_n|$.

Remark: We note that if $(\delta_j)_{j=1,\ldots,n}$ denotes the error affecting x_j-values and $F(x_j) = y_j$, then it follows

$$F(x_j + \delta_j) = F(x_j) + \underbrace{F'(x_j)\delta_j + \mathcal{O}(\delta_j^2)}_{\epsilon_j} = y_j + \epsilon_j = y_j \left(1 + \frac{\epsilon_j}{F(x_j)}\right) \ (F(x_j) \neq 0),$$

i.e. a perturbation δ_j on x_j-values reflects upon a perturbation ϵ_j on y_j-values and vice versa. Hence, for simplicity of notations, the sensitivity analysis only analyzes how the error introduced on y_j propagates, assuming that there is no perturbation on x_j-values.

We assume that

$$y^\theta_j = y_j(1 + \theta_j), \quad \text{where} \quad |\theta_j| \leqslant \theta,$$

are noisy Lt values and $s_\theta(x)$ is the generalized complete smoothing spline obtained from (x_j, y^θ_j). We denote by $(\alpha^f_2)^\theta$ and $(\alpha^f_n)^\theta$ the values of α^f_2 and α^f_n corresponding to y^θ_i, respectively, by $(S^1_L)^\theta$ and $(S^1_R)^\theta$ the values of S^1_L and S^1_R corresponding to y^θ_i and by z^θ and c^θ the vectors defined in (55) and in (56) corresponding to y^θ_i.

The following theorem summarizes the propagation error analysis of $\mathcal{P}_1$.

Theorem 5.1. *Let c be the solution of system (55); it holds*

$$\frac{\|c - c^\theta\|_\infty}{\|c\|_\infty} \leqslant \mu_\infty(B + \rho E) \frac{\theta}{h_{\min}} k_{\theta, y, \Delta_n}, \tag{57}$$

where $h_{\min}$ is as in (22), k_{θ,y,Δ_n} is as in (67) and

$$\mu_\infty(B + \rho E) = \|B + \rho E\|_\infty \|(B + \rho E)^{-1}\|_\infty. \tag{58}$$

To prove this result we first demonstrate the following three lemmas.

Lemma 5.2. *For $j = 2, \ldots, n$, it holds*

$$|(\alpha^f_j)^\theta - \alpha^f_j| \leqslant \frac{2\theta}{h_j} x^{\zeta_{f,r}}_{j-1} \left(1 + \mathcal{O}\left(\theta^2\right)\right) (1 + \zeta_{f,r}\mathcal{O}(h_j)). \tag{59}$$

Proof. From the definition of α^f_j in (16) and from that of $(\alpha^f_j)^\theta$, if $f \equiv r$, it holds

$$|(\alpha^r_j)^\theta - \alpha^r_j| = \left|\frac{\ln((1 + \theta_{j-1})/(1 + \theta_j))}{\ln(x_j/x_{j-1})}\right| = \left|\frac{\ln(1 + \theta_{j-1}) - \ln(1 + \theta_j))}{\ln(x_j/x_{j-1})}\right|$$

and from (33)

$$= \left| \frac{\theta_{j-1} + O(\theta_{j-1}^2) - \theta_j + O(\theta_j^2)}{\frac{h_j}{x_{j-1}} - \frac{h_j^2}{x_{j-1}^2} + o(h_j^2)} \right| \leqslant \frac{2\theta + 2O(\theta^2)}{\frac{h_j}{x_{j-1}} - \frac{h_j^2}{x_{j-1}^2} + o(h_j^2)}.$$

Finally, by using the Taylor series of the power function

$$\phi(z) = (1+z)^{-1} = (1 - z + O(z^2)) \quad (z \to 0),$$

we obtain

$$\begin{aligned} |(\alpha_j^r)^\theta - \alpha_j^r| &\leqslant (2\theta + 2O(\theta^2)) \frac{x_{j-1}}{h_j} \left[1 - \frac{1}{2} \frac{h_j}{x_{j-1}} + o(h_j) \right] \\ &\leqslant (2\theta + 2O(\theta^2)) \frac{x_{j-1}}{h_j} \left[1 + \mathcal{O}(h_j) \right]. \end{aligned}$$

If $f \equiv e$, then it follows

$$|(\alpha_j^e)^\theta - \alpha_j^e| = \left| \frac{\ln(y_{j-1}^\theta / y_j^\theta)}{h_j} - \frac{\ln(y_{j-1}/y_j)}{h_j} \right| \leqslant \frac{2\theta + 2O(\theta^2)}{h_j}.$$

□

Lemma 5.3. *It holds*

$$|(S_L^1)^\theta - S_L^1| \leqslant 2\theta \frac{|y_1|}{h_2} \left\{ \left(1 + \mathcal{O}(\theta^2)\right) (1 + \zeta_{f,r} \mathcal{O}(h_j)) + |\ln(y_1/y_2)| \right\}, \tag{60}$$

$$|(S_R^1)^\theta - S_R^1| \leqslant 2\theta \frac{|y_n|}{h_n} \left\{ \left(1 + \mathcal{O}(\theta^2)\right) (1 + \zeta_{f,r} \mathcal{O}(h_j)) + |\ln(y_{n-1}/y_n)| \right\}. \tag{61}$$

Proof. Let us consider $(S_L^1)^\theta - S_L^1$. From (19) we have

$$\begin{aligned} \left(S_L^1\right)^\theta - S_L^1 &= -\left(\alpha_2^f\right)^\theta y_1^\theta \gamma_f\left(x_1, -\zeta_{f,r}\right) + \alpha_2^f y_1 \gamma_f\left(x_1, -\zeta_{f,r}\right) \\ &= \gamma_f\left(x_1, -\zeta_{f,r}\right)\left(\alpha_2^f y_1 - (\alpha_2^f)^\theta y_1^\theta\right). \end{aligned} \tag{62}$$

By adding and subtracting $\gamma_f(x_1, -\zeta_{f,r})\alpha_2^f y_1^\theta$ and using (59) and (16), we obtain

$$\begin{aligned} |(S_L^1)^\theta - S_L^1| &\leqslant \gamma_f(x_1, -\zeta_{f,r})\left(|(\alpha_2^f)^\theta - \alpha_2^f||y_1^\theta| + |\alpha_2^f||y_1 - y_1^\theta|\right) \\ &\leqslant \frac{2\theta}{h_2}(1 + \mathcal{O}(\theta^2))(1 + \zeta_{f,r}\mathcal{O}(h_j))|y_1|(1+\theta) + \gamma_f(x_1, -\zeta_{f,r})\alpha_2^f||y_1|\theta \\ &\leqslant 2\theta \frac{|y_1|}{h_2}\{(1 + O(\theta^2))(1 + \zeta_{f,r}\mathcal{O}(h_j)) + |\ln(y_1/y_2)|\}. \end{aligned} \tag{63}$$

In the same way, if we consider $(S_R^1)^\theta - S_R^1$, from (19) we have

$$\begin{aligned} (S_R^1)^\theta - S_R^1 &= -(\alpha_n^f)^\theta y_n^\theta \gamma_f(x_n, -\zeta_{f,r}) + \alpha_n^f y_n \gamma_f(x_n, -\zeta_{f,r}) \\ &= \gamma_f(x_n, -\zeta_{f,r})(\alpha_n^f y_n - (\alpha_n^f)^\theta y_n^\theta) \end{aligned} \tag{64}$$

by adding and subtracting $\gamma_f(x_n, -\zeta_{f,r})\alpha_n^f y_n^\theta$, and using (59) and (16), it follows

$$\begin{aligned} |(S_R^1)^\theta - S_R^1| &\leqslant \gamma_f(x_n, -\zeta_{f,r})\left(|(\alpha_n^f)^\theta - \alpha_n^f||y_n^\theta| + |\alpha_n^f||y_n - y_n^\theta|\right) \\ &\leqslant \frac{2\theta}{h_n}(1 + \mathcal{O}(\theta^2))(1 + \zeta_{f,r}\mathcal{O}(h_j)) + |y_n|(1+\theta) + \gamma_f(x_n, -\zeta_{f,r})\alpha_n^f||y_n|\theta \\ &\leqslant 2\theta \frac{|y_n|}{h_n}\{(1 + \mathcal{O}(\theta^2))(1 + \zeta_{f,r}\mathcal{O}(h_j)) + |\ln(y_{n-1}/y_n)|\}. \end{aligned} \tag{65}$$

□

Lemma 5.4. *Let z be as in (55) and (56); it holds*

$$\frac{\|z - z^\theta\|_\infty}{\|z\|_\infty} \leqslant \frac{\theta}{h_{\min}} k_{\theta,y,\Delta_n}, \tag{66}$$

where $h_{\min}$ is as in (22) and

$$k_{\theta,y,\Delta_n} = \max \left\{ \begin{array}{l} (2\left(1+\mathcal{O}(\theta^2)\right)(1+\zeta_{f,r}\mathcal{O}(h_j)) + |\ln(y_1/y_2)|), \\ (2\left(1+\mathcal{O}(\theta^2)\right)(1+\zeta_{f,r}\mathcal{O}(h_j)) + |\ln(y_{n-1}/y_n)|) \end{array} \right\}. \tag{67}$$

Proof. From (60) it follows

$$\begin{aligned} \|z - z^\theta\|_\infty &= \max(|(S_L^1)^\theta - S_L^1|, |y_1|\theta, \ldots, |y_n|\theta, \ldots, |(S_R^1)^\theta - S_R^1|) \\ &\leqslant \max(\theta\|y\|_\infty, |(S_L^1)^\theta - S_L^1|, |(S_R^1)^\theta - S_R^1|) \leqslant \theta\|y\|_\infty \frac{k_{\theta,y,\Delta_n}}{\min(h_2, h_n)}. \end{aligned} \tag{68}$$

Combining (68) with $\|z\|_\infty^{-1} \leqslant \|y\|_\infty^{-1}$, we obtain the thesis. □

Concerning problem $\mathcal{P}_2$, if $\mathcal{K}_{2m,p}$ is the condition number of the $2m$th-order B-splines, computed with respect to the L_p norm ($1 \leqslant p \leqslant \infty$), then in [21] it is proved that

$$\mathcal{K}_{2m,p} < 2m2^{2m}, \tag{69}$$

where

$$\frac{\|\sum c_j^\theta \hat{N}_j^{2m} - \sum c_j \hat{N}_j^{2m}\|_{L_p}}{\|\sum c_j \hat{N}_j^{2m}\|_{L_p}} \leqslant \mathcal{K}_{2m,p} \frac{\|c^\theta - c\|_{l_p}}{\|c\|_{l_p}} \quad \forall \hat{N}_j^{2m}, c, c^\theta \tag{70}$$

and

$$\hat{N}_j^{2m} = (2m/(\tau_{j+2m} - \tau_j))^{1/p} N_j^{2m}$$

denote the $2m$th-order B-splines normalized with respect to the L_p-norm ($1 \leqslant p \leqslant \infty$). In particular, if $p = \infty$ and $m = 2$ we obtain the following.

Theorem 5.5. *It holds*

$$\frac{\max_{x\in[x_1,x_n]} |s_\theta(x) - s(x)|}{\max_{x\in[x_1,x_n]} |s(x)|} < 64\mu_\infty(B + \rho E)\frac{\theta}{h_{\min}} k_{\theta,y,\Delta_n}, \tag{71}$$

where $h_{\min}$ is as in (22) and k_{θ,y,Δ_n} is as in (67).

Proof. The thesis follows from (57), (69) and (70). □

Remark. If $\rho = 0$, then $\mu_\infty(B + \rho E) = \mu_\infty(B)$. Numerical simulations show that $\mu_\infty(B)$ depends on $\|\Delta_n\|$ and that it exponentially grows as m. The best case occurs if $\forall k \; x_k - x_{k-1} = \|\Delta_n\| \equiv \delta$ and $m = 2$. Then

$$B = \begin{bmatrix} -3/\delta & 3/\delta & 0 & & & & & & \\ 1 & 0 & 0 & & & & & & \\ 0 & 1/4 & 7/12 & 1/6 & & & & & \\ & & 1/6 & 2/3 & 1/6 & & & & \\ & & & \ddots & \ddots & \ddots & & & \\ & & & & 1/6 & 2/3 & 1/6 & & \\ & & & & & 1/6 & 7/12 & 1/4 & \\ & & & & & & 0 & 0 & 1 \\ & & & & & & 0 & 3/\delta & -3/\delta \end{bmatrix} \tag{72}$$

and a straightforward computation shows that if $\delta \leqslant 3$, $\|B^{-1}\|_\infty < 4$, $\|B\|_\infty < 6/\delta$, and $\mu_\infty(B) < 24/\delta$.

If $\rho \neq 0$, $\mu_\infty(B + \rho E)$ worsens since matrix E is ill-conditioned.

The last result concerns the propagation error analysis on $[x_n, \infty)$.

Theorem 5.6. *If $x \geqslant x_n$, it holds*

$$\widetilde{\psi}(x) = |s_\theta(x) - s(x)| \leqslant |y_n|\theta \max\left\{1, \frac{2\,(1+\mathcal{O}(\theta))}{|\ln(y_{n-1}/y_n)|}\right\}. \tag{73}$$

In order to demonstrate this result we need the following.

Lemma 5.7. *If $\theta_{n-1} = \theta_n$ the function $\widetilde{\psi}(x)$ has a global maximum at $x = x_n$. If $\theta_{n-1} \neq \theta_n$ the function $\widetilde{\psi}(x)$ has a local maximum at $\bar{x} = \left(\frac{\alpha_n^f \beta_n^f}{(\alpha_n^f)^\theta (\beta_n^f)^\theta}\right)^{\frac{1}{\alpha_n^f - (\alpha_n^f)^\theta}}$.*

Proof. Let us assume that $\theta_{n-1} = \theta_n$; then from (16) and (17), $(\alpha_n^f)^\theta = \alpha_n^f$ and $(\beta_n^f)^\theta = \beta_n^f$.

It holds

$$s_\theta(x) = s_{(\alpha_n^f)^\theta} \equiv s_{\alpha_n^f}.$$

On $[x_n, \infty)$, it is

$$s_{\alpha_n^f} \equiv \beta_n^f \cdot \gamma_f(x, -\alpha_n^f).$$

Then, it follows that

$$\widetilde{\psi}(x) = |s_\theta(x) - s(x)| = |y_n^\theta \cdot \gamma_f(x, -\alpha_n^f) - y_n \cdot \gamma_f(x, -\alpha_n^f)| = |(y_n^\theta - y_n) \cdot \gamma_f(x, -\alpha_n^f)|$$

which is a decreasing function on $[x_n, \infty)$, because γ_f is a decreasing function. Hence $\widetilde{\psi}(x_n)$ is its global maximum on $[x_n, \infty)$.

Otherwise, if $\theta_{n-1} \neq \theta_n$, we have

$$\widetilde{\psi}(x) = |s_\theta(x) - s(x)| = |(\beta_n^f)^\theta \cdot \gamma_f(x, -(\alpha_n^f)^\theta) - \beta_n^f \cdot \gamma_f(x, -\alpha_n^f)|$$

and a unique local maximum of ψ can be found at $\bar{x} = \left(\frac{\alpha_n^f \beta_n^f}{(\alpha_n^f)^\theta (\beta_n^f)^\theta}\right)^{\frac{1}{\alpha_n^f - (\alpha_n^f)^\theta}}$ if $f = r$ or at $\bar{x} = \ln\left(\frac{\alpha_n^f \beta_n^f}{(\alpha_n^f)^\theta (\beta_n^f)^\theta}\right)^{\frac{1}{\alpha_n^f - (\alpha_n^f)^\theta}}$ if $f = e$. □

Now we demonstrate theorem 5.7.

Proof. We consider two cases.

(i) If $\theta_{n-1} = \theta_n$, by lemma 5.7, $\widetilde{\psi}(x_n)$ is a global maximum of $\widetilde{\psi}(x)$; hence,

$$\widetilde{\psi}(x) \leqslant \widetilde{\psi}(x_n) = |y_n^\theta - y_n| \leqslant |y_n|\theta. \tag{74}$$

(ii) If $\theta_{n-1} \neq \theta_n$, by lemma 5.7,

$$\widetilde{\psi}(x) \leqslant \widetilde{\psi}(\bar{x}).$$

From (16) and (17)

$$\begin{aligned}
\widetilde{\psi}(\bar{x}) &= \left|\frac{\beta_n^f \gamma_f(\bar{x}, (\alpha_n^f)^\theta - \alpha_n^f) - (\beta_n^f)^\theta}{\gamma_f(\bar{x}, (\alpha_n^f)^\theta)}\right| = \left|\frac{\beta_n^f \frac{(\alpha_n^f)^\theta (\beta_n^f)^\theta}{\alpha_n^f \beta_n^f} - (\beta_n^f)^\theta}{\gamma_f(\bar{x}, (\alpha_n^f)^\theta)}\right| \\
&\leqslant \frac{|(\beta_n^f)^\theta|}{\gamma_f(x_n, (\alpha_n^f)^\theta)} \left|\frac{(\alpha_n^f)^\theta - \alpha_n^f}{\alpha_n^f}\right| \\
&= |y_n^\theta| \left|\frac{(\alpha_n^f)^\theta - \alpha_n^f}{\alpha_n^f}\right| = |y_n^\theta| \left|\frac{|\ln((1+\theta_{n-1}|)/(1+\theta_n))}{|\ln(y_{n-1}/y_n)|}\right| \\
&\leqslant |y_n|(1+\theta)\frac{2\theta + \mathcal{O}(\theta^2)}{|\ln(y_{n-1}/y_n)|} = |y_n|\theta\frac{2\,(1+\mathcal{O}(\theta))}{|\ln(y_{n-1}/y_n)|}.
\end{aligned}$$

Hence, in this case

$$\widetilde{\psi}(\bar{x}) \leqslant |y_n|(1+\theta)\frac{2\theta + \mathcal{O}(\theta^2)}{|\ln(y_{n-1}/y_n)|} = |y_n|\theta\frac{2\,(1+\mathcal{O}(\theta))}{|\ln(y_{n-1}/y_n)|}. \tag{75}$$

Finally, collecting (74) and (75) we obtain

$$\psi(x) \leqslant \max\left\{|y_n|\theta, |y_n|\theta\frac{2\,(1+\mathcal{O}\,(\theta))}{|\ln(y_{n-1}/y_n)|}\right\}.$$

□

6. Experimental results

In this section, we report some experiments aimed to show the usefulness of the fitting model. In particular, we analyze

(i) how a Lt function is approximated by the generalized smoothing spline (section 6.1),
(ii) how much the inverse function of the generalized smoothing spline differs from the Lt inverse function (section 6.2),
(iii) how the generalized smoothing spline compares with another fitting spline (section 6.3).

We fix $d = 3$ and increase both the number of nodes needed to construct the spline and the variance σ^2 of the data error distribution.

6.1. Experimental results on the Laplace transform approximation

Results show that the distance between the smoothing spline and the Lt function is bounded below and, in particular, the following.

(i) Given a fixed number of data samples n, the approximation error decreases as the variance decreases. Furthermore, results obtained for the interpolating model ($\rho = 0$) agree with the ones obtained in experiments 1 and 2;.
(ii) Given a fixed $\sigma \neq 0$, the approximation error decreases as the number of samples grows.

We describe results obtained in $[x_1, \infty)$, both for approximating a Lt function with rational decay (test 6.1.1) and for approximating a Lt function with exponential decay (test 6.1.2). All experiments are carried out using the MATLAB package. As already said (see experiments 1 and 2 of section 4), following [1], we consider two data point distributions: uniform and geometric. As is known, in both cases the Lt is uniquely specified when its values are given at points forming such distributions [1]. The approximation error is computed using the maximum error E_∞:

$$E_\infty = \|s_\rho - F\|_{l^\infty} = \max_{i=1,\ldots,101} |s_\rho(p_i) - F(p_i)|$$

computed on 101 points geometrically or uniformly distributed on a prescribed interval.

Test 6.1.1. Laplace transform with a rational decay. Nodes uniformly distributed. Let

$$(x_i, \tilde{y}_i), \qquad i = 1, \ldots, n,$$

be a set of noisy values of

$$F(x) = 2x/(1+x^2)^2,$$

where noise is normally distributed with zero mean and variance σ^2:

$$y_i = F(x_i), \qquad \tilde{y}_i = y_i(1+e_i), \quad < e_i >= 0, \quad \sigma(e_i) = \overline{\sigma}.$$

By using

$$n \in \{5, 20, 30, 40, 60, 80, 100\},$$

we construct the generalized smoothing spline using the rational end behavior model on

$$\Delta_n = \{x_1, \ldots, x_n\}, \qquad \text{where} \qquad x_1 = a = 0.1, \qquad x_n = b = 14.6$$

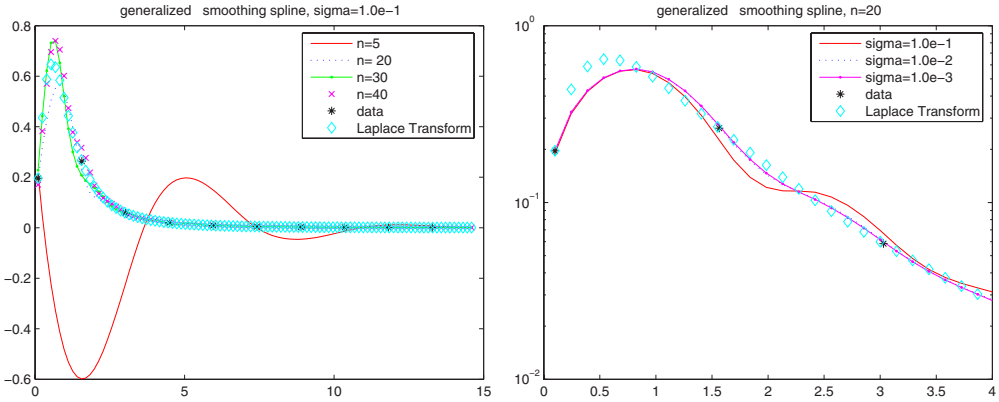

Figure 3. Left: plot of the Lt $(x, F(x))$ and of the generalized smoothing spline for $n = [5,\ 10,\ 20,\ 30,\ 40]$, $\sigma = 1.0 \times 10^{-1}$. $x \in [0, 15]$. Right: plot of the Lt $(x, F(x))$ and of the generalized smoothing spline for $n = 20$ and $\sigma = 1.0 \times 10^{-1}, 1.0 \times 10^{-2}, 1.0 \times 10^{-3}$. $x \in [0.1, 4]$.

Table 1. E_∞ on $[a, b] = [0.1, 14.6]$, generalized polynomial smoothing spline.

$\sigma \backslash n$	5	10	20	30	40
10^{-1}	9.9923e–001	4.2219e–001	1.4253e–001	4.2149e–002	7.2332e–002
10^{-2}	8.8428e–001	4.2040e–001	1.5624e–001	5.4008e–002	2.8534e–002
10^{-3}	8.7414e–001	4.2023e–001	1.5763e–001	5.7915e–002	3.0993e–002
10^{-4}	8.7314e–001	4.2021e–001	1.5777e–001	5.8306e–002	3.1239e–002
10^{-5}	8.7304e–001	4.2021e–001	1.5778e–001	5.8345e–002	3.1264e–002
0	8.7303e–001	4.2021e–001	1.5779e–001	5.8349e–002	3.1266e–002
$\sigma \backslash n$	60	80	100	120	
10^{-1}	1.0529e–001	9.5005e–002	8.0289e–002	1.0270e–001	
10^{-2}	1.0561e–002	9.4072e–003	8.0311e–003	1.0271e–002	
10^{-3}	9.2272e–003	2.4809e–003	8.1221e–004	1.0284e–003	
10^{-4}	9.4492e–003	2.4110e–003	1.0409e–004	4.8525e–004	
10^{-5}	9.4714e–003	2.4040e–003	4.9164e–005	4.5311e–004	
0	9.4738e–003	2.4032e–003	5.4099e–005	4.4954e–004	

and x_j are uniformly distributed between x_1 and x_n. Moreover, we set

$$w_L = 1; \quad w_R = 1; \quad \rho = \sigma^2/n.$$

Table 1 shows E_∞ computed on 101 points uniformly distributed on [0.1, 14.6] for different values of n and σ. Figures 3 and 4 show results.

Observe that for $\sigma = 0$ and $n = 30$, it results that E_∞ is just the maximum of the E_j, $j = 1, \ldots, n-1$, computed in experiment 1.

Table 2 and figures 5 and 6 are concerned with the generalized smoothing spline approximation in $[x_n, +\infty)$. In particular, E_∞ on [14.6, 20] is shown.

Observe that for $\sigma = 0$ and $n = 30$, E_∞ is *comparable* with E_n computed in the experiment 1.

Test 6.1.2. Laplace transform with exponential decay. Nodes geometrically distributed. Let us consider the set

$$(x_i, \tilde{y}_i), \quad i = 1, \ldots, n,$$

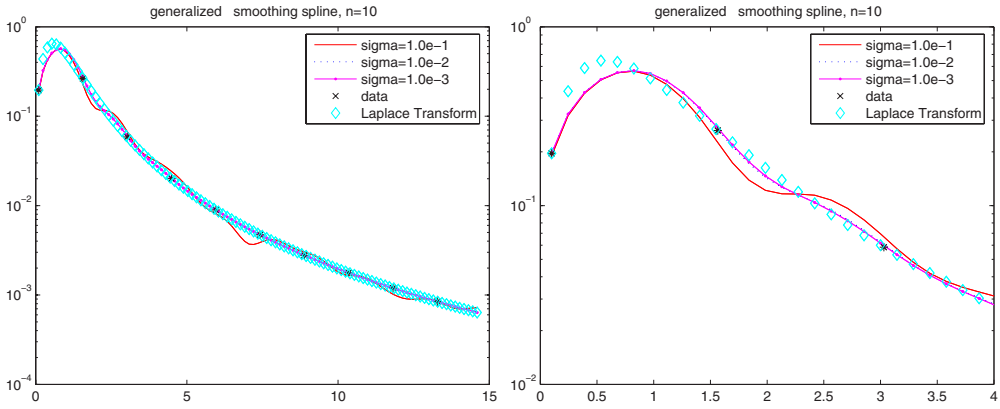

Figure 4. Plot of the Lt $(x, F(x))$ and of the generalized smoothing spline: $n = 10$, $\sigma = 1.0 \times 10^{-1},\ 1.0 \times 10^{-2},\ 1.0 \times 10^{-3}$, y-log scale. Left: $x \in [0, 15]$. Right: $x \in [0.1, 4]$.

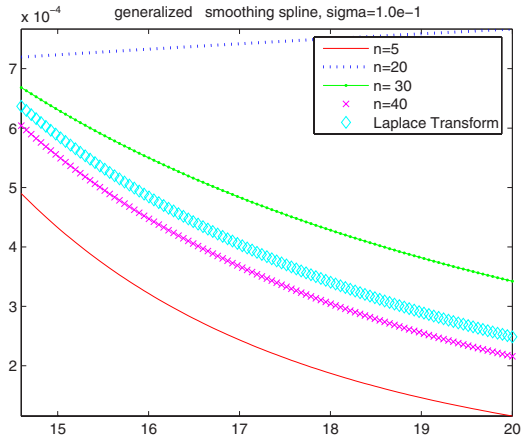

Figure 5. Plot of the Lt $(x, F(x))$ and of the generalized smoothing spline, $x \in [15, 20]$, $n = [5,\ 10,\ 20,\ 30,\ 40]$ and $\sigma = 1.0 \times 10^{-1}$.

Table 2. E_∞ on [14.6, 20].

$\sigma \backslash n$	5	20	30	40	60	80	100
10^{-1}	1.63e–04	5.18e–04	9.35e–05	3.71e–05	1.58e–03	2.38e–04	4.14e–04
10^{-2}	1.31e–05	3.12e–05	8.65e–06	3.83e–06	5.60e–05	3.75e–05	9.43e–05
10^{-3}	1.29e–06	3.38e–06	1.24e–06	3.50e–07	5.47e–06	3.68e–06	1.08e–05
10^{-4}	7.75e–07	7.48e–07	5.09e–07	3.78e–07	9.04e–07	1.67e–07	8.09e–07
10^{-5}	8.73e–07	4.86e–07	4.36e–07	4.11e–07	4.51e–07	3.54e–07	2.77e–07
0	8.83e–07	4.57e–07	4.28e–07	4.14e–07	4.01e–07	3.95e–07	3.91e–07

of the noisy values of

$$F(x) = \mathrm{e}^{-x}/(1 + x),$$

where noise is normally distributed with zero mean and variance σ^2.

We construct the generalized smoothing spline using the exponential end behavior model on the data set

$$\Delta_n = \{x_1, \ldots, x_n\}, \qquad \text{where} \qquad x_1 = a = 5, \qquad x_n = b = 20$$

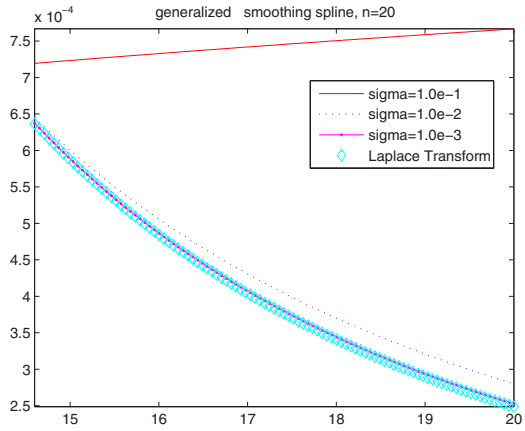

Figure 6. Plot of the Lt $(x, F(x))$ and of the generalized smoothing spline, $x \in [15, 20]$, $n = 20$, $\sigma = 1.0 \times 10^{-1},\ 1.0 \times 10^{-2},\ 1.0 \times 10^{-3}$.

Table 3. E_∞ on [5, 20].

$\sigma \backslash n$	5	20	30	40	60	80	100
10^{-1}	1.03e–04	7.44e–05	2.86e–04	2.85e–04	8.10e–04	1.69e–03	8.41e–03
10^{-2}	4.37e–05	8.83e–06	1.66e–05	1.65e–05	1.94e–05	1.50e–05	1.81e–05
10^{-3}	3.90e–05	2.75e–07	1.37e–07	7.97e–08	3.58e–08	2.02e–08	1.29e–008
10^{-4}	3.91e–05	2.54e–07	2.93e–07	1.63e–07	1.5895e–07	1.16e–07	1.41e–07
10^{-5}	3.90e–05	2.73e–07	1.53e–07	7.10e–08	4.46e–08	2.47e–08	1.42e–08
0	3.90e–05	2.75e–07	1.37e–07	7.97e–08	3.58e–08	2.02e–08	1.29e–08

Table 4. E_∞ on [20, 30].

$\sigma \backslash n$	5	20	30	40	60	80	100
10^{-1}	2.54e+00	1.26e−11	4.97e−12	5.05e−12	1.19e−11	7.81e−12	2.70e−11
10^{-2}	1.14e−11	1.26e−12	4.77e−13	5.31e−13	1.02e−12	8.26e−13	2.86e−12
10^{-3}	5.01e−13	1.26e−13	6.50e−14	8.99e−14	7.71e−14	1.29e−13	3.15e−13
10^{-4}	3.28e−13	9.43e−14	8.10e−14	7.59e−14	5.91e−14	6.86e−14	7.97e−14
10^{-5}	3.20e−13	1.00e−13	8.28e−14	7.47e−14	6.58e−14	6.32e−14	6.22e−14
0	3.20e−13	1.01e−13	8.30e−14	7.46e−14	6.65e−14	6.27e−14	6.04e−14

by choosing the nodes distributed between x_1 and x_n as follows:

$$x_{i+1} = x_i \cdot (b/a)^{1/(n-1)} \qquad i = 1, ..., n-1.$$

Moreover, we set

$$w_L = 1; \quad w_R = 1; \quad \rho = \sigma^2/n.$$

In table 3, we report E_∞ for different n and σ. Figures 7 and 8 show the results.

Observe that for $\sigma = 0$ and $n = 30$, it results that E_∞ is just the maximum of the $E_j,\ j = 1, \ldots, n-1$, computed in experiment 2.

Table 4 and figures 9 and 10 are concerned with the generalized smoothing spline approximation in $[x_n, +\infty)$. In particular, E_∞ computed on 101 points geometrically distributed on [20, 30] is shown.

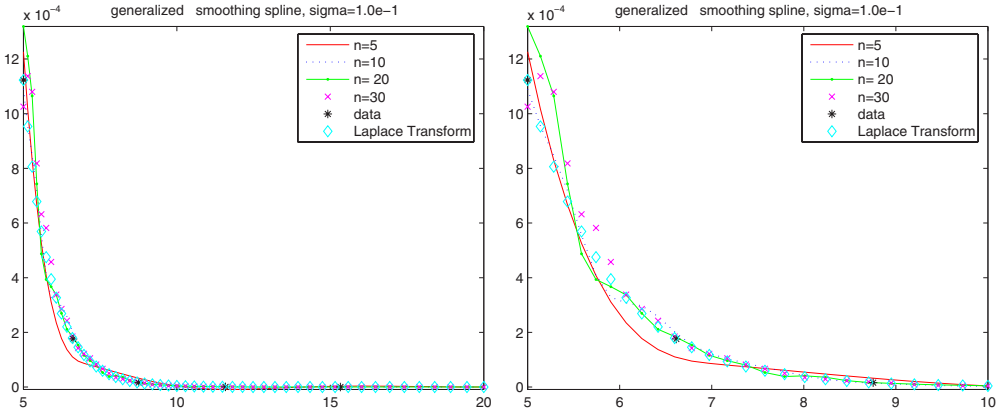

Figure 7. Plot of the Lt $(x, F(x))$ and of the generalized smoothing spline: $n = [5,\ 10,\ 20,\ 30]$, $\sigma = 1.0 \times 10^{-1}$. Left: $x \in [5, 20]$. Right: $x \in [5, 10]$.

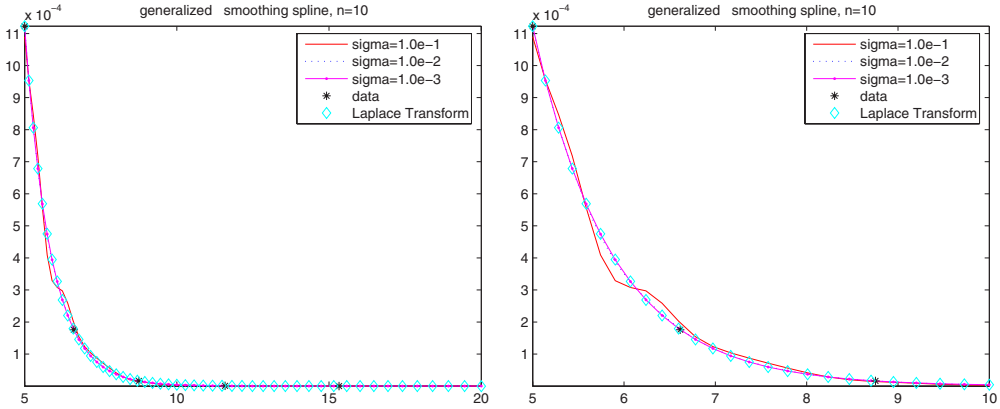

Figure 8. Plot of the Lt $(x, F(x))$ and of the generalized smoothing spline: $n = 10$, $\sigma = 1.0 \times 10^{-1},\ 1.0 \times 10^{-2},\ 1.0 \times 10^{-3}$, y-log scale. Left: $x \in [5, 20]$. Right: $x \in [5, 10]$.

Observe that for $\sigma = 0$ and $n = 30$, E_∞ is just E_n computed in experiment 2. As expected, the approximation provided by the generalized smoothing spline is ever more accurate as the number of samples grows and agrees with the error variance σ on data samples. Of course, the approximation error is much smaller on $[x_n, +\infty)$ due to the asymptotic decay of the Lt function.

6.2. Numerical inversion

In this section we discuss experimental results obtained by inverting the generalized smoothing spline. We construct the generalized interpolating spline ($\rho = 0$) because we assume that data (x_i, y_i), $i = 1, \ldots, n$ belong to a known Lt function. By this way, to investigate how much the inverse function of the spline, $f_s(t)$, differs from that obtained inverting the Lt function, i.e. $f_F(t)$, is straightforward. We consider the Stehfest algorithm [23], available in the MATLAB package, and the Pike's algorithm [29].

We analyze how much the inverse function of the generalized smoothing spline, f_s, differs from the inverse function of the Lt, f_F. To this aim, to measure the difference between the

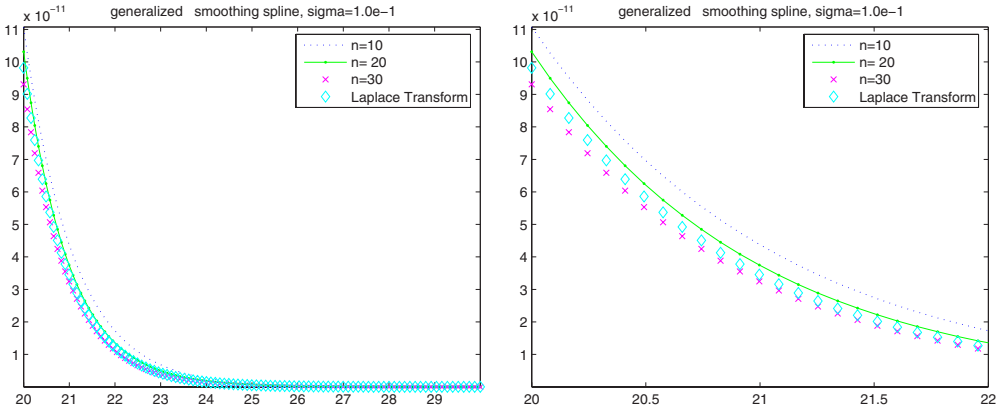

Figure 9. Plot of the Lt $(x, F(x))$ and of the generalized smoothing spline for $n = [10,\ 20,\ 30]$, and $\sigma = 1.0 \times 10^{-1}$. Left: $x \in [20, 30]$. Right: $x \in [20, 22]$.

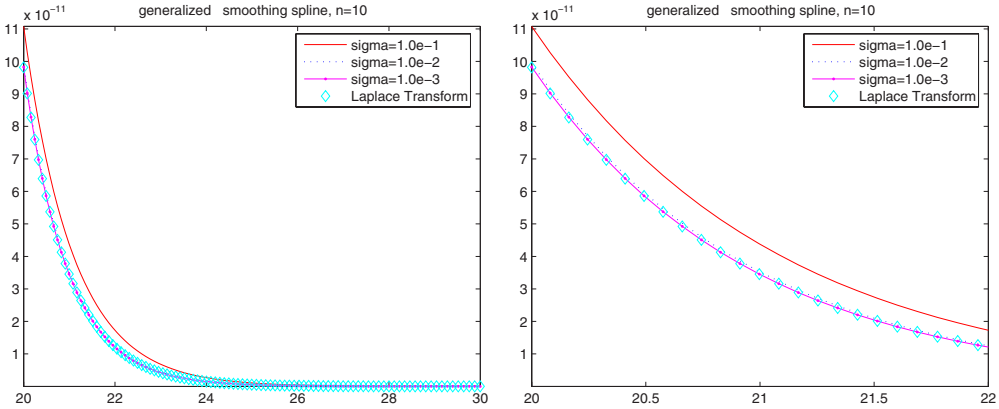

Figure 10. Plot of the Lt $(x, F(x))$ and of the generalized smoothing spline for $n = 10$, $\sigma = 1.0 \times 10^{-1},\ 1.0 \times 10^{-2},\ 1.0 \times 10^{-3}$. Left: $x \in [20, 30]$. Right: $x \in [20, 22]$.

inverse functions, f_s and f_F, we use the relative error:

$$|f_F(t) - f_s(t)|/|f_F(t)|$$

computed at $t \equiv t_i$ where $t_i = 1, 2, 3, \ldots, 10$. Instead, taking into account that the Lt is an integral operator, to measure the overall difference between the Lt function and the generalized smoothing spline, in this case it is more suitable to use the root mean square error of prediction (RMSEP), which is computed as follows:

$$\text{RMSEP} = \sqrt{\frac{\sum_{i=1,\ldots,P} \left(\frac{s_F(p_i) - F(p_i)}{F(p_i)} \right)^2}{P}}, \qquad P = 101.$$

The P points p_i, $i = 1, \ldots, P$, are uniformly distributed on an interval $[c, d]$, which is chosen such that it contains the evaluation points of the input function (the Lt function or the generalized smoothing spline) needed by the inversion algorithm for computing the inverse function at t_i.

Table 5. RMSEP on $[c, d] = [0.06931, 2.7724]$.

$\sigma \backslash n$	10	20	40	60	80
0	1.1628e–002	4.0902e–003	3.3309e–003	3.2127e–003	3.1602e–003
$\sigma \backslash n$	100	120			
0	3.1304e–003	3.1108e–003			

Table 6. $f_F(t)$ versus $f_s(t)$, $n = 20$, $M = 4$.

t	f_F	f_s	$\lvert f_F - f_s\rvert$	$\lvert f_F - f_s\rvert/\lvert f_F\rvert$
1	3.3878e–001	3.9361e–001	5.4824e–002	1.6183e–001
2	1.3709e–001	1.3718e–001	8.2675e–005	6.0305e–004
3	6.4971e–002	6.4293e–002	6.7776e–004	1.0432e–002
4	3.4067e–002	3.2805e–002	1.2611e–003	3.7017e–002
5	1.9060e–002	1.6001e–002	3.0588e–003	1.6049e–001
6	1.1097e–002	1.8527e–002	7.4298e–003	6.6952e–001
7	6.5884e–003	2.1541e–002	1.4952e–002	2.2695e+000
8	3.9080e–003	1.2306e–002	8.3983e–003	2.1490e+000
9	2.2550e–003	−2.5265e–003	4.7815e–003	2.1204e+000
10	1.2072e–003	−1.3609e–002	1.4816e–002	1.2273e+001

We construct the generalized smoothing spline assuming a uniform data distribution on the interval:

$$x_1 = 0.05, \qquad x_n = 2 \quad (n = 10, 20, 40, ..., 120).$$

Test 6.2.1 [23].

$$F(x) = 1/(1 + x), \qquad f(t) = \mathrm{e}^{-t}$$

taking into account that at $M = 4$ the Stehfest algorithm evaluates the smoothing spline and the Lt function on

$$[c, d], \qquad \text{where} \qquad c = 0.069\,31, \qquad d = 4 \times 0.6931 = 2.7724$$

we compute the RMSEP on $[c, d]$. Tables 5 and 6 report results obtained by using the Stehfest algorithm (using $M = 4$ terms) to compute the inverse functions (f_F and f_s) of the Laplace function F and the inverse function of the generalized smoothing spline s_F, respectively. We note that if $n \geqslant 40$ RMSEP does not change significantly, then we only show inversion results at $n = 20, 40$.

In figures 11 and 12, we compare f_F and f_s at $t = 1, \ldots, 10$.

Test 6.2.2 [29].

$$F(x) = 1/(1 + x)^2, \qquad f(t) = t\mathrm{e}^{-t},$$

taking into account that we use $M = 4$, in this case the interval $[c, d]$ is $[0.069\,31, 2.7724]$. From table 7, we note that if $n \geqslant 40$ RMSEP does not change significantly. Therefore, for numerical inversion we only show results obtained using $n = 20, 40$.

Tables 8 and 9 report results obtained by using the Stehfest algorithm to compute the inverse functions (f_F and f_s) of the Laplace function F and of smoothing spline s_F, respectively.

In figures 13 and 14, we compare f_F and f_s at $t = 1, \ldots, 10$.

Test 6.2.3 [23].

$$F(x) = 1/x^4, \qquad f(t) = t^3/6;$$

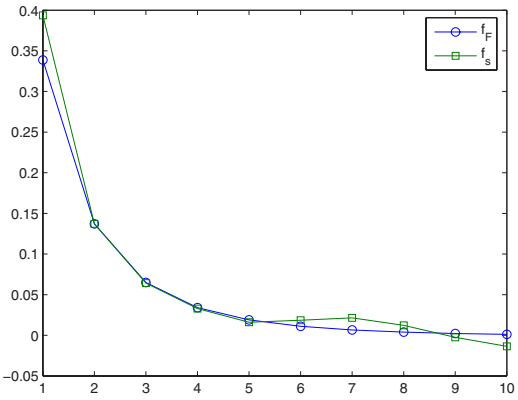

Figure 11. Test 1. $M = 4$, $t = 1, \ldots, 10$. $n = 20$.

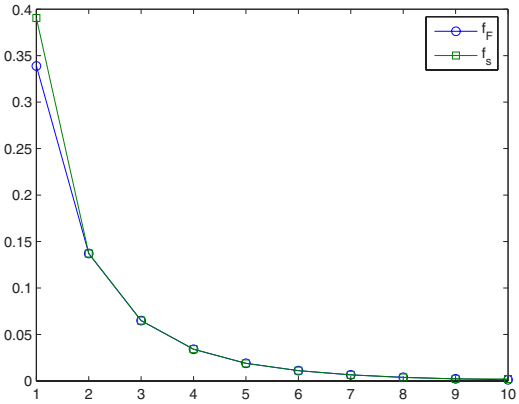

Figure 12. Test 1. $M = 4$, $t = 1, \ldots, 10$. $n = 40$.

Table 7. $f_F(t)$ versus $f_s(t)$, $n = 40$, $M = 4$.

t	f_F	f_s	$\lvert f_F(t) - f_s\rvert$	$\lvert f_F - f_s\rvert/\lvert f_F$
1	3.3878e–001	3.9042e–001	5.1636e–002	1.5242e–001
2	1.3709e–001	1.3709e–001	3.6471e–007	2.6603e–006
3	6.4971e–002	6.4949e–002	2.1745e–005	3.3469e–004
4	3.4067e–002	3.4145e–002	7.8268e–005	2.2975e–003
5	1.9060e–002	1.8901e–002	1.5880e–004	8.3317e–003
6	1.1097e–002	1.1041e–002	5.5902e–005	5.0375e–003
7	6.5884e–003	6.5774e–003	1.0939e–005	1.6603e–003
8	3.9080e–003	3.7626e–003	1.4548e–004	3.7226e–002
9	2.2550e–003	2.3348e–003	7.9713e–005	3.5349e–002
10	1.2072e–003	2.1649e–003	9.5767e–004	7.9328e–001

taking into account that we use $M = 4$, in this case the interval $[c, d]$ is $[0.069\,31, 6 \cdot 0.6931$ $(= 4.1589)]$. From table 10 we observe that if $n \geqslant 100$ RMSEP does not change significantly, thus we choose to only show inversion results obtained using $n = 100, 120$ to construct s_F.

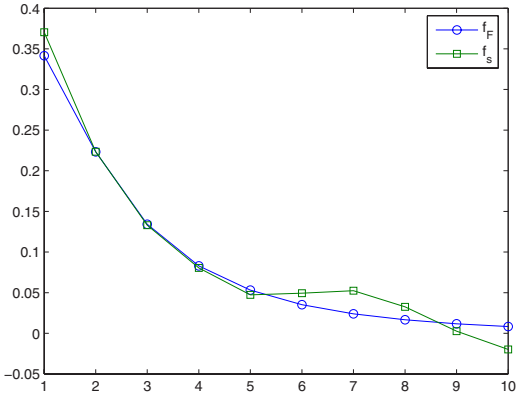

Figure 13. Test 2. $M = 4$: $f_F(t)$ versus $f_s(t)$, $t = 1, \ldots, 10$. $n = 20$.

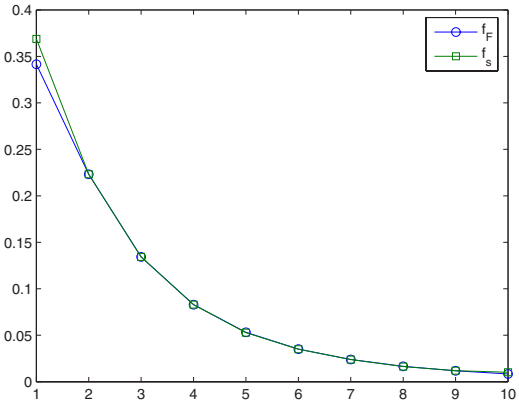

Figure 14. Test 2. $M = 4$: $f_F(t)$ versus $f_s(t)$, $t = 1, \ldots, 10$. $n = 40$.

Table 8. RMSEP on $[c, d] = [0.06931, 2.7724]$.

$\sigma \backslash n$	10	20	40	60	80
0	2.5633e–002	8.3017e–003	6.6939e–003	6.4545e–003	6.3485e–003
$\sigma \backslash n$	100	120			
0	6.2883e–003	6.2488e–003			

Table 9. $f_F(t)$ versus $f_s(t)$, $n = 20$, $M = 4$.

t	f_F	f_s	$\lvert f_F(t) - f_s(t)\rvert$	$\lvert f_F(t) - f_s(t)\rvert / \lvert f_F(t)\rvert$
1	3.4159e–001	3.7036e–001	2.8770e–002	8.4225e–002
2	2.2320e–001	2.2335e–001	1.5756e–004	7.0592e–004
3	1.3425e–001	1.3296e–001	1.2879e–003	9.5932e–003
4	8.2896e–002	8.0500e–002	2.3966e–003	2.8911e–002
5	5.3101e–002	4.7283e–002	5.8181e–003	1.0957e–001
6	3.5149e–002	4.9299e–002	1.4150e–002	4.0257e–001
7	2.3897e–002	5.2380e–002	2.8483e–002	1.1919e+000
8	1.6590e–002	3.2585e–002	1.5995e–002	9.6416e–001
9	1.1698e–002	2.5963e–003	9.1014e–003	7.7805e–001
10	8.3367e–003	−1.9877e–002	2.8214e–002	3.3843e+000

Table 10. $f_F(t)$ versus $f_s(t)$, $n = 40$, $M = 4$.

t	f_F	f_s	$\lvert f_F(t) - f_s(t)\rvert$	$\lvert f_F(t) - f_s(t)\rvert/\lvert f_F(t)\rvert$
1	3.4159e–001	3.6879e–001	2.7195e–002	7.9613e–002
2	2.2320e–001	2.2320e–001	7.1356e–007	3.1970e–006
3	1.3425e–001	1.3421e–001	4.1499e–005	3.0911e–004
4	8.2896e–002	8.3046e–002	1.4959e–004	1.8046e–003
5	5.3101e–002	5.2798e–002	3.0274e–004	5.7012e–003
6	3.5149e–002	3.5042e–002	1.0725e–004	3.0512e–003
7	2.3897e–002	2.3876e–002	2.0832e–005	8.7174e–004
8	1.6590e–002	1.6312e–002	2.7761e–004	1.6734e–002
9	1.1698e–002	1.1851e–002	1.5285e–004	1.3067e–002
10	8.3367e–003	1.0160e–002	1.8236e–003	2.1874e–001

Table 11. RMSEP on $[c, d] = [0.06\,931, 4.1589]$.

$\sigma \backslash n$	10	20	40	60	80
0	8.8529e+002	1.5921e+001	2.7908e–001	3.6301e–002	1.0477e–002
$\sigma \backslash n$	100	120	140	150	160
0	4.4485e–004	9.0253e–004	4.8961e–004	2.8390e–004	1.2562e–004

Table 12. $f_F(t)$ versus $f_s(t)$, $n = 100$, $M = 6$.

t	f_F	f_s	$\lvert f_F(t) - f_s(t)\rvert$	$\lvert f_F(t) - f_s(t)\rvert/\lvert f_F(t)\rvert$
1	5.7690e–001	5.7690e–001	3.4615e–006	6.0001e–006
2	4.6152e+000	4.6153e+000	8.1841e–005	1.7733e–005
3	1.5576e+001	1.5579e+001	2.5002e–003	1.6051e–004
4	3.6922e+001	3.6720e+001	2.0202e–001	5.4715e–003
5	7.2113e+001	6.9815e+001	2.2980e+000	3.1867e–002
6	1.2461e+002	1.3121e+002	6.5953e+000	5.2927e–002
7	1.9788e+002	1.7411e+002	2.3769e+001	1.2012e–001
8	2.9537e+002	3.1536e+002	1.9987e+001	6.7667e–002
9	4.2056e+002	4.7075e+002	5.0192e+001	1.1935e–001
10	5.7690e+002	6.2533e+002	4.8430e+001	8.3949e–002

Tables 11 and 12 report results obtained by using the Stehfest algorithm (using $M = 6$) to compute the original function (f_F and f_s) by using as input function the Laplace function F and the smoothing spline s_F.

Test 6.2.4 [29]. We invert the Laplace function of test 6.2.2:

$$F(s) = \frac{1}{(1+x)^2}, \quad f(t) = te^{-t}$$

by using Pike's algorithm [29]. We construct the generalized smoothing spline assuming uniform data distribution in

$$x_1 = 10^{-15}, \qquad x_n = 3 \quad (n = 10, 20, 40, ..., 120).$$

Following [29], the interval $[c, d]$ is $[10^{-15}, 10^5]$. To measure the difference between the Lt function and the generalized smoothing spline, taking into account the length of the interval $[c, d]$, in this case it is more reliable to use root-mean-square error (RMSE)

$$\text{RMSE} = \sqrt{\frac{\sum_{i=1,...,N} (s_F(p_i) - F(p_i))^2}{N}}, \qquad N = 101.$$

Table 13. $f_F(t)$ versus $f_s(t)$, $n = 120$, $M = 6$.

t	f_F	f_s	$\lvert f_F(t) - f_s(t)\rvert$	$\lvert f_F(t) - f_s(t)\rvert/\lvert f_F(t)\rvert$
1	5.7690e–001	5.7690e–001	6.2585e–007	1.0848e–006
2	4.6152e+000	4.6152e+000	1.2732e–006	2.7588e–007
3	1.5576e+001	1.5577e+001	2.1861e–004	1.4035e–005
4	3.6922e+001	3.6917e+001	5.1386e–003	1.3917e–004
5	7.2113e+001	7.2333e+001	2.1993e–001	3.0498e–003
6	1.2461e+002	1.2461e+002	1.7068e–003	1.3697e–005
7	1.9788e+002	1.9767e+002	2.0865e–001	1.0544e–003
8	2.9537e+002	2.8658e+002	8.7962e+000	2.9780e–002
9	4.2056e+002	4.4135e+002	2.0786e+001	4.9423e–002
10	5.7690e+002	5.9718e+002	2.0277e+001	3.5148e–002

Table 14. RMSE on $[c, d] = [10^{-15}, 10^5]$.

$\sigma \backslash n$	10	20	40	60
0	1.1858e–006	1.0945e–006	1.0569e–006	1.0453e–006
$\sigma \backslash n$	80	100	120	
0	1.0397e–006	1.0364e–006	1.0342e–006	

Table 15. $f_F(t)$ versus $f_s(t)$, $n = 10$.

t	f_F	f_s	$\lvert f_F(t) - f_s(t)\rvert$	$\lvert f_F(t) - f_s(t)\rvert/\lvert f_F(t)\rvert$
0.5	2.9759e–001	2.3422e–001	6.3368e–002	2.1294e–001
1	3.7399e–001	4.7184e–001	9.7856e–002	2.6166e–001
1.5	3.3430e–001	3.4077e–001	6.4792e–003	1.9382e–002
2	2.6561e–001	2.0443e–001	6.1188e–002	2.3037e–001
2.5	2.0082e–001	1.2417e–001	7.6651e–002	3.8170e–001
3	1.4800e–001	8.6508e–002	6.1490e–002	4.1548e–001
3.5	1.0730e–001	7.2896e–002	3.4399e–002	3.2060e–001
4	7.6736e–002	7.0721e–002	6.0151e–003	7.8386e–002
4.5	5.4111e–002	7.2777e–002	1.8666e–002	3.4496e–001

Table 16. $f_F(t)$ versus $f_s(t)$, $n = 20$.

t	f_F	f_s	$\lvert f_F(t) - f_s(t)\rvert$	$\lvert f_F(t) - f_s(t)\rvert/\lvert f_F(t)\rvert$
0.5	2.9759e–001	2.7151e–001	2.6078e–002	8.7631e–002
1	3.7399e–001	3.9151e–001	1.7519e–002	4.6845e–002
1.5	3.3430e–001	3.5162e–001	1.7328e–002	5.1835e–002
2	2.6561e–001	2.7235e–001	6.7410e–003	2.5379e–002
2.5	2.0082e–001	1.9835e–001	2.4622e–003	1.2261e–002
3	1.4800e–001	1.3982e–001	8.1818e–003	5.5283e–002
3.5	1.0730e–001	9.6430e–002	1.0866e–002	1.0127e–001
4	7.6736e–002	6.5334e–002	1.1403e–002	1.4859e–001
4.5	5.4111e–002	4.3535e–002	1.0576e–002	1.9545e–001

In table 13, we see that the RMSE does not change significantly if $n \geqslant 40$. Hence, we only show inversion results when the generalized smoothing spline is constructed at $n = 10, 20, 40$. In tables 14–17, we compare results obtained running the Pike algorithm on F and on the generalized smoothing spline s_F constructed using $n = 10, 20, 40$ knots. Following [29], t-values are $t \equiv t_i$ where $t_i = 0.5 + 0.5 \cdot i$, $i = 0, \ldots, 8$. In figures 15–16 we compare f_f and f_s at $t = 1, \ldots, 10$. In figures 17–19, we compare numerical values of the inverse functions f_F and f_S.

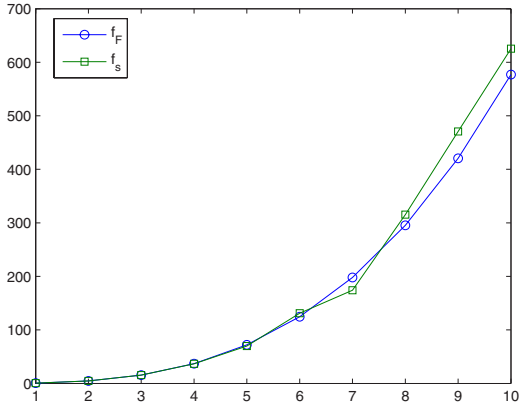

Figure 15. Test 3. $M = 6$, $f_F(t)$ versus $f_s(t)$, $t = 1, \ldots, 10$. $n = 100$.

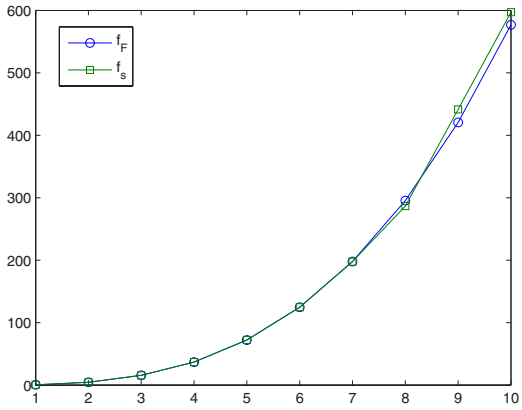

Figure 16. Test 3. $M = 6$, $f_F(t)$ versus $f_s(t)$, $t = 1, \ldots, 10$. $n = 120$.

Table 17. $f_F(t)$ versus $f_s(t)$, $n = 40$.

t	f_F	f_s	$\lvert f_F(t) - f_s(t)\rvert$	$\lvert f_F(t) - f_s(t)\rvert / \lvert f_F(t)\rvert$
0.5	2.9759e–001	2.7764e–001	1.9950e–002	6.7040e–002
1.	3.7399e–001	3.9738e–001	2.3399e–002	6.2565e–002
1.5	3.3430e–001	3.4180e–001	7.4996e–003	2.2434e–002
2.	2.6561e–001	2.6091e–001	4.7045e–003	1.7712e–002
2.5	2.0082e–001	1.9219e–001	8.6267e–003	4.2958e–002
3.	1.4800e–001	1.4004e–001	7.9582e–003	5.3773e–002
3.5	1.0730e–001	1.0176e–001	5.5321e–003	5.1559e–002
4.	7.6736e–002	7.3908e–002	2.8280e–003	3.6853e–002
4.5	5.4111e–002	5.3624e–002	4.8676e–004	8.9956e–003

Table 18. E_∞ on [0.1, 14.6], generalized exponential spline.

$\sigma \backslash n$	5	10	20	30	40
0	8.1085e–001	4.2138e–001	1.5903e–001	5.8707e–002	3.1363e–002
$\sigma \backslash n$	60	80	100	120	
0	9.4880e–003	2.4034e–003	5.3993e–005	4.4775e–004	

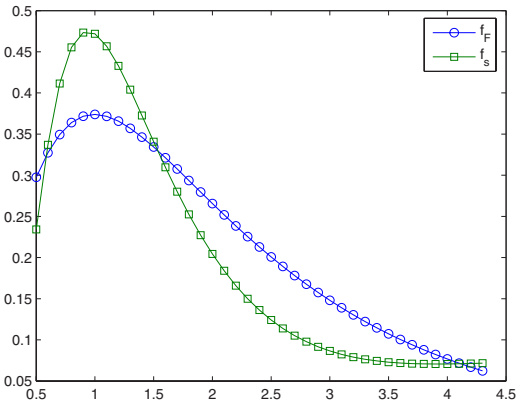

Figure 17. Test 4. $f_F(t)$ versus $f_s(t)$. $n = 10$.

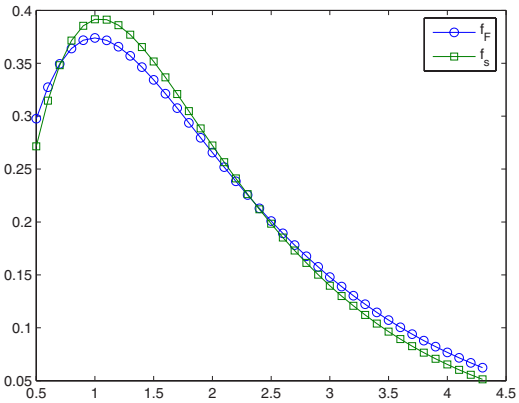

Figure 18. Test 4. $f_F(t)$ versus $f_s(t)$. $n = 20$.

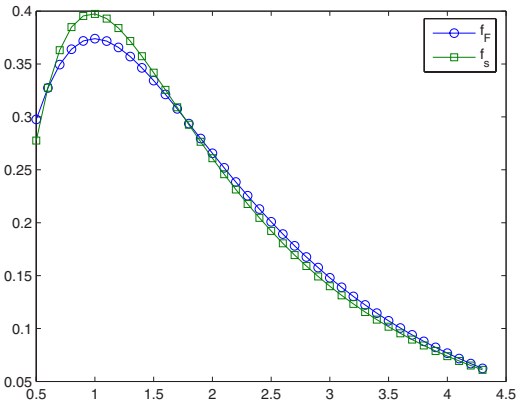

Figure 19. Test 4. $f_F(t)$ versus $f_s(t)$. $n = 40$.

Table 19. E_∞ on [0.1, 14.6], generalized polynomial spline.

$\sigma \backslash n$	5	10	20	30	40
0	8.7303e–001	4.2021e–001	1.5779e–001	5.8349e–002	3.1266e–002
$\sigma \backslash n$	60	80	100	120	
0	9.4738e–003	2.4032e–003	5.4099e–005	4.4954e–004	

Table 20. E_∞ on $[c, d] = [14.6, 20]$, generalized exponential spline.

$\sigma \backslash n$	5	10	20	30	40
0	8.8340e–007	5.6063e–007	4.5730e–007	4.2817e–007	4.1443e–007
$\sigma \backslash n$	60	80	100	120	
0	4.0121e–007	3.9478e–007	3.9098e–007	3.8847e–007	

Table 21. E_∞ on [14.6, 20], generalized polynomial spline.

$\sigma \backslash n$	5	10	20	30	40
0	8.8340e–007	5.6063e–007	4.5730e–007	4.2817e–007	4.1443e–007
$\sigma \backslash n$	60	80	100	120	
0	4.0121e–007	3.9478e–007	3.9098e–007	3.8847e–007	

Table 22. E_∞ on [5, 20], generalized exponential spline.

$\sigma \backslash n$	5	10	20	30	40
0	5.2553e–006	1.1168e–006	3.3229e–007	1.4231e–007	8.3323e–008
$\sigma \backslash n$	60	80	100	120	
0	2.9758e–008	8.5057e–009	2.1234e–010	1.9249e–009	

Table 23. E_∞ on [5, 20], generalized polynomial spline.

$\sigma \backslash n$	5	10	20	30	40
0	3.8994e–005	1.3205e–006	2.7079e–007	1.3367e–007	7.9751e–008
$\sigma \backslash n$	60	80	100	120	
0	2.9041e–008	8.3990e–009	2.1211e–010	1.9418e–009	

Table 24. E_∞ on $[c, d] = [20, 30]$, generalized exponential spline.

$\sigma \backslash n$	5	10	20	30	40
0	3.2000e–013	1.6304e–013	1.0109e–013	8.3061e–014	7.4583e–014
$\sigma \backslash n$	60	80	100	120	
0	6.6540e–014	6.2712e–014	6.0433e–014	5.8974e–014	

Table 25. E_∞ on $[c, d] = [20, 30]$, generalized polynomial spline.

$\sigma \backslash n$	5	10	20	30	40
0	3.2000e–013	1.6304e–013	1.0109e–013	8.3061e–014	7.4583e–014
$\sigma \backslash n$	60	80	100	120	
0	6.6540e–014	6.2712e–014	6.0433e–014	5.8974e–014	

Table 26. E_∞ on [0.05, 2], generalized exponential spline.

$\sigma \backslash n$	5	10	20	30	40
0	1.7794e–001	4.5138e–002	1.1950e–002	5.2385e–003	3.1560e–003
$\sigma \backslash n$	60	80	100	120	
0	1.1642e–003	3.3852e–004	8.5249e–006	7.7673e–005	

Table 27. E_∞ on [0.05, 2], generalized polynomial spline.

$\sigma \backslash n$	5	10	20	30	40
0	1.7927e–001	4.5200e–002	1.1954e–002	5.2391e–003	3.1562e–003
$\sigma \backslash n$	60	80	100	120	
0	1.1642e–003	3.3853e–004	8.5251e–006	7.7674e–005	

Table 28. E_∞ on $[c, d] = [2, 20]$, generalized exponential spline.

$\sigma \backslash n$	5	10	20	30	40
0	3.0281e–002	2.6789e–002	2.5542e–002	2.5177e–002	2.5003e–002
$\sigma \backslash n$	60	80	100	120	
0	2.4835e–002	2.4752e–002	2.4703e–002	2.4671e–002	

Table 29. E_∞ on $[c, d] = [2, 20]$, generalized polynomial spline.

$\sigma \backslash n$	5	10	20	30	40
0	3.0281e–002	2.6789e–002	2.5542e–002	2.5177e–002	2.5003e–002
$\sigma \backslash n$	60	80	100	120	
0	2.4835e–002	2.4752e–002	2.4703e–002	2.4671e–002	

Table 30. E_∞ on [0.05, 2], generalized exponential spline.

$\sigma \backslash n$	5	10	20	30	40
0	3.4153e–001	8.6146e–002	2.2774e–002	9.9798e–003	6.0121e–003
$\sigma \backslash n$	60	80	100	120	
0	2.2176e–003	6.4481e–004	1.6238e–005	1.4794e–004	

Table 31. E_∞ on [0.05, 2], generalized polynomial spline.

$\sigma \backslash n$	5	10	20	30	40
0	3.4418e–001	8.6269e–002	2.2781e–002	9.9810e–003	6.0126e–003
$\sigma \backslash n$	60	80	100	120	
0	2.2177e–003	6.4483e–004	1.6238e–005	1.4795e–004	

From these results we can say that the generalized smoothing spline mimics well the Lt function. Indeed, the inverse function approximates the original inverse function and also the generalized smoothing spline provides a better approximation of the Lt function.

6.3. Comparisons between the generalized polynomial smoothing spline and the generalized exponential smoothing spline

In this section, we compare the approximation errors on the Lt function provided by the generalized polynomial smoothing spline and by the generalized exponential smoothing spline. The generalized exponential smoothing spline was developed using exponential splines

Table 32. E_∞ on $[c, d] = [2, 10]$, generalized exponential spline.

$\sigma \backslash n$	5	10	20	30	40
0	7.1384e–003	6.0201e–003	5.6261e–003	5.5114e–003	5.4568e–003
$\sigma \backslash n$	60	80	100	120	
0	5.4039e–003	5.3780e–003	5.3627e–003	5.3525e–003	

Table 33. E_∞ on $[c, d] = [2, 10]$, generalized polynomial spline.

$\sigma \backslash n$	5	10	20	30	40
0	7.1384e–003	6.0201e–003	5.6261e–003	5.5114e–003	5.4568e–003
$\sigma \backslash n$	60	80	100	120	
0	5.4039e–003	5.3780e–003	5.3627e–003	5.3525e–003	

(as described in [22]), inside the knot intervals, and the end behavior models (rational or exponential) outside. To construct the exponential splines we set all tension parameters equal to 1.

Approximation errors are computed on $[x_1, x_n]$, the interval containing the knots used to construct the generalized smoothing splines, and on the interval $[c, d] \supset [x_1, x_n]$. The approximation errors are computed evaluating the maximum error E_∞,

$$E_\infty = \max_{i=1,\ldots,P} |s_\rho(p_i) - F(p_i)|,$$

on 101 points uniformly distributed at the prescribed intervals. For test cases 1 and 2, intervals $[x_1, x_n]$ and $[c, d]$ are chosen as in the previous approximations tests (see sections 6.1); for test cases 3 and 4, $[x_1, x_n]$ is the same as in the inversion tests (see section 6.2), while $[c, d]$ is slightly greater than that used in the inversion tests because here we are interested in analyzing the overall approximation error.

Furthermore, to construct the generalized (polynomial/exponential) smoothing spline we employ the rational end behavior model in all test cases except in test 2, where we use the exponential end behavior model. Finally, we assume that the knots x_i, $i = 1, \ldots, n$, are uniformly distributed in all test cases except in test 2, where we use a geometric data distribution.

Test 6.3.1.

$$F(x) = 2x/(1 + x^2)^2.$$

Test 6.3.2.

$$F(x) = \mathrm{e}^{-x}/(1 + x).$$

Test 6.3.3.

$$F(x) = 1/(1 + x).$$

Test 6.3.4.

$$F(x) = 1/(1 + x)^2.$$

In tables 18–21 we report the approximation error for test 6.3.1, in tables 22–25 we consider the test function 6.3.2. Finally, tables 26–29 refer to test 6.3.3 and tables 30–33 to test 6.3.4. We note that in $[x_1, x_n]$ the approximation errors are quite the same. In $[c, d]$, the generalized smoothing spline provides a better approximation of the Lt function than the exponential spline.

7. Conclusions and future work

We address the real inversion problem of a Laplace transform function which is only known on a finite set of measurements. More precisely, the paper focuses on the construction of a generalized polynomial smoothing spline for approximating Laplace transform functions only known at a finite set of measurements along the real axis. Starting from the data set, we construct a generalized polynomial spline defined on the whole real line, which is a complete polynomial smoothing spline inside the data interval while it enjoys Laplace transform properties outside the data interval. We address both the rational decay end behavior and the exponential decay end behavior. The selection of the end decay model may be done according to a priori information on data or on the behavior of the inverse function at zero. We show results concerning existence and uniqueness, and we give approximation error bounds.

Furthermore, in order to investigate how much the inverse function of the spline differs from the original function, we report experimental results obtained by running two real inversion algorithms (the Stehfest algorithm and the Pike algorithm). We compare results obtained by employing the smoothing spline as an input function to the inversion algorithms with the numerical values of the original function obtained by using the Laplace transform function. We observe that the generalized smoothing spline mimics well the Laplace transform function: the approximation of the inverse function improves and also the generalized smoothing spline provides a better approximation of the Laplace transform.

Finally, we compare the approximation provided by the generalized polynomial smoothing spline with the same obtained by using exponential splines inside the knot intervals. Numerical results confirm that approximation errors are quite the same. The authors plan to implement the related numerical algorithm that takes into account both polynomial and exponential splines inside and outside the knot intervals. The selection of the fitting model may be done according to *a priori* information on data.

Acknowledgments

The authors are grateful to the anonymous referees who made helpful comments, improving the quality of the paper.

References

[1] Bertero M, Brianzi P and Pike E R 1985 On the recovery and resolution of exponential relaxation rates from experimental data: III. The effect of sampling and truncation of data on the Laplace transform inversion *Proc. R. Soc.* A **398** 23–44

[2] Borgia G C, Brown R J S and Fantazzini P 2000 Uniform penalty inversion of multiexponential decay data: II *J. Magn. Reson.* **147** 273–85

[3] Campagna R, D'Amore L, Galletti A, Murli A and Rizzardi M 2010 *On the Numerical Approximation of the Laplace Transform Function from Real Samples and Its Inversion* (*Numerical Mathematics and Advanced Applications 2009*) ed G Kreiss *et al* (Berlin: Springer) pp 209–16

[4] Chiu Li Hu and Schumaker Larry L 1986 Complete spline smoothing *Numer. Math.* **49** 1–10

[5] Craven P and Wahba G 1979 Smoothing noisy data with spline functions. Estimating the correct degree of smoothing by the method of generalized cross-validation *Numer. Math.* **31** 377–403

[6] de Boor C 1978 *A Practical Guide to Splines* (New York: Springer)

[7] Faure P F and Rodts S 2008 Proton NMR relaxation as a probe for setting cement pastes *Magn. Reson. Imaging* **26** 1183–96

[8] Forsyth G E 1957 Generation and the use of orthogonal polynomials for data fitting with a digital computer *J. Soc. Ind. Appl. Math.* **5** 74–88

[9] Kounchev O 2001 *Multivariate Polysplines. Applications to Numerical and Wavelet Analysis* (New York: Academic)

[10] Kimeldorf G and Wahba G 1970 A correspondence between Bayesian estimation on stochastic processes and smoothing by splines *Ann. Math. Stat.* **41** 495–502
[11] Micchelli C 1976 Cardinal L-splines studies *Spline Functions and Approximation Theory* ed S Karlin, C Micchelli, A Pinkus and I J Shoenberg (New York: Academic) pp 203–50
[12] Montella C, Michel R and Diard J P 2007 Numerical inversion of Laplace transforms: a useful tool for evaluation of chemical diffusion coefficients in ion-insertion electrodes investigated by PITT *J. Electroanal. Chem.* **608** 37–46
[13] O'Hagan A and C Kingman J F 1978 Curve fitting and optimal design for prediction *J. R. Stat. Soc.* B **40** (1) 1–42
[14] Provencher S W 1982 A Constrained regularization method for inverting data represented by linear algebraic or integral equations *Comput. Phys. Commun.* **27** 213–27
[15] Reinsch C H 1967 Smoothing by spline functions *Numer. Math.* **10** 177–83
[16] Savitzky A and Golay Marcel J E 1964 Smoothing and differentiation of data by simplified least-squares procedures *Anal. Chem.* **36** 1627–39
[17] Schoenberg I J 1964 On interpolation by spline functions and its minimal properties *On Approximation Theory* (*Proc. of Oberwolfach Conf. 1963*) ISNM vol 5 ed P L Butzer and J Korevaar (Basel: Birkauser) pp 109–29
[18] Schoenberg I J 1964 Spline functions and the problem of graduation *Proc. Natl Acad. Sci. USA* **52** 947–50
[19] Schoenberg I J 1973 *Cardinal Interpolation* (Providence, RI: American Mathematical Society)
[20] Schumaker Larry L 1981 *Spline Functions: Basic Theory* (New York: Wiley)
[21] Sherer K and Yu Shadrin A 1999 New upper bound for the B-spline basis condition number *J. Approx. Theory* **99** 217–29
[22] Späth H 1969 Exponential spline interpolation *Computing* **4** 225–33
[23] Stehfest H 1970 Algorithm 368: numerical inversion of Laplace transforms *Commun. ACM* **13** 47–49
[24] Stoer J 1974 *Introduzione all'analisi numerica* (Bologna: Zanichelli)
[25] Velleman P F 1980 Definition and comparison of robust nonlinear data smoothing algorithms *J. Am. Stat. Assoc.* **75** 609–15
[26] Wahba G 1978 Improper priors, spline smoothing and the problem of guarding against model errors in regression *J. R. Stat. Soc.* B **40** (3) 364–72
[27] Wahba G 1990 *Spline Models for Observational Data* (*CBMS-NSF Regional Conference Series in Applied Mathematics* vol 59) (Philadelphia: SIAM)
[28] Whittaker E T 1922 On a new method of graduation *Proc. Edinburgh Math. Soc.* **41** 63–75
[29] Whirter J G and Pike E R 1978 On the numerical inversion of the Laplace transform and similar Fredholm integral equations of the first kind *J. Phys. A Math. Gen.* **11** 1729–45
[30] Winter D A, Sidwall H G and Hobson D A 1974 Measurement and reduction of noise in kinematics of locomotion *J. Biomech.* **7** 157–9
[31] van der Weerd L, Melnikov S M, Vergeldt F J, Novikov E G and Van As H 2002 Modelling of self-diffusion and relaxation time NMR in multicompartment systems with cylindrical geometry *J. Magn. Reson.* **156** 213–21
[32] Zhao X 2004 An efficient approach for the numerical inversion of Laplace transform and its application in dynamic fracture analysis of a piezoelectric laminate *Int. J. Solids Struct.* **41** 3653–74